Meteorological Applications of Satellite Indirect Soundings

Department of Meteorology
University of Wisconsin–Madison
1225 W. Dayton Street
Madison, Wisconsin 53706

Contributions by

L. H. Horn
A. F. Kapela
R. A. Petersen
T. M. Whittaker

L. H. Horn, Principal Investigator

PROJECT REPORT

The research in this report has been supported
by the National Environmental Satellite Service of the
National Oceanic and Atmospheric Administration under Grant 04-4-158-2

August 1975

Meteorological Applications of Satellite Indirect Soundings

Department of Meteorology
University of Wisconsin—Madison
1225 W. Dayton Street
Madison, Wisconsin 53706

Contributions by

L. H. Horn
A. F. Kapela
R. A. Petersen
T. M. Whittaker

L. H. Horn, Principal Investigator

PROJECT REPORT

The research in this report has been supported
by the National Environmental Satellite Service of the
National Oceanic and Atmospheric Administration under Grant 04-4-158-2

August 1975

Table of Contents

1. Introduction

The research presented in this report consists of work done with support of NOAA Grant 04-4-158-2 during the period August 1973 through August 1975. During much of the first year of this period only limited amounts of Nimbus-5 data were available. Consequently, most of the work presented here was done during the latter part of the two year period.

The major goal of this research has been to employ temperature profiles derived from infrared and microwave observations made from polar orbiting satellites in a number of synoptic and dynamic studies. Because the satellite indirect sounding technique provides a radically new source of data for the meteorological community, it is important that these data be used in a variety of studies. Such work is warranted in two respects: 1) the studies can serve to assess the quality of the satellite data and 2) the structure of the atmosphere can be examined for the first time in regions where conventional radiosonde data are lacking. Although the two are not mutually exclusive, the major initial thrust has been directed toward the first. Since the satellite soundings are very new it is important that studies be done in areas which are rich in conventional radiosonde data so that comparisons are possible. Until the characteristics and general quality of the satellite data are determined, their employment in remote areas must be rather limited.

Because the scan mechanism of Nimbus-5 Infrared Temperature Profile Radiometer malfunctioned shortly after launch, the work presented here has concentrated on vertical cross sectional analyses of the atmosphere. In order to put the satellite data to a severe test we focused on cross sections through especially strong baroclinic zones located in regions where excellent

radiosonde data were also available. Our initial work, as represented by the article by Kapela and Horn, employed conventional subjective cross sectional analyses. Although the meteorologist can draw on a great deal of experience in subjectively analyzing cross sectional data and can achieve considerable insight into the quality of the data, the process is so time-consuming that only limited studies are possible. To circumvent this difficulty a computer program was developed by Whittaker and Petersen, which not only objectively analyzes the isentropic field but also calculates the wind field normal to the cross section using both the observed rawinsonde winds and the thermal field. The program, which has greatly facilitated studies employing cross sectional analyses, is described in the second paper.

In the final paper by Horn, Petersen and Whittaker, the objective analysis program was employed to achieve intercomparisons between cross sections based on Nimbus-5 soundings, rawinsonde data, and the initialized data of the Limited Area Fine Mesh model of NMC. The results show that properly selected Nimbus-5 data are capable of resolving the thermal field in an intense baroclinic field and should be suitable for inclusion in numerical models if the data are inserted in an optimum way. In particular it appears that the best results will be achieved by inserting gradients rather than absolute values of the data.

The members of the research project gratefully acknowledge the support provided by the National Environmental Satellite Service (NESS). Dr. William L. Smith and Dr. Christopher Hayden of NESS were especially helpful in providing the Nimbus-5 data and encouragement during the past two years.

Lyle H. Horn
Principal Investigator
August, 1975

Nimbus-5 Satellite Soundings in a Strongly Baroclinic Region

Anton F. Kapela and Lyle H. Horn

Department of Meteorology, University of Wisconsin-Madison, Wisconsin 53706

Abstract

Isentropic cross sections based on both conventional radiosonde and Nimbus-5 infrared (ITPR) and microwave (NEMS) sounding data have been constructed through an intense baroclinic zone. Temperature gradients from the cross sections and 850 mb geostrophic winds have been used to obtain geostrophic wind components normal to the cross sections. Because the flow was cyclonically curved, gradient wind components were also calculated. The results show that, for the most part, gradient wind estimates obtained from Nimbus-5 measurements compare favorably with values obtained from radiosonde thermal gradients. In general, the RMS differences between gradient winds derived from the Nimbus-5 data and observed (rawin) winds are slightly smaller than the RMS differences between radiosonde derived gradient winds and observed winds.

1. Introduction

Since the existence of the jet stream was confirmed by high flying aircraft during World War II, the synoptic meteorologist has been greatly interested both in its location and that of the local wind maxima (jet streaks) which propagate along it. The patterns of convergence and divergence produced by the propagating jet streaks are often instrumental in initiating cyclogenesis and outbreaks of severe weather. In regions with excellent rawinsonde coverage, such as the United States, existing wind observations are often adequate to delineate a jet streak. At other times, however, the observations from these stations, typically 400-500 km apart, are insufficient to resolve the extent and strength of the jet maxima. In such situations the synoptician can often enhance the available observational data by analyzing vertical cross sections. The rich vertical detail of the wind and temperature variations provided by a rawinsonde ascent can be used to better resolve the horizontal thermal gradients. These temperature gradients and the thermal wind relationship can then provide a description of the wind field which is greatly enhanced over that obtained from wind observations alone. See for example, Newton (1954), Danielson (1959), Duquet, Danielson and Phares (1964), and Cahir (1971).

Recently, Togstad and Horn (1974) investigated the possibility of using temperature profiles obtained from satellite irradiance measurements to construct isentropic cross sections which describe the thermal gradients beneath a jet streak. Employing rawinsonde observations from five stations, they analyzed an isentropic cross section through an actual jet streak. From this cross section, they extracted synthetic temperature soundings, and from these computed corresponding theoretical infrared irradiances at 1° latitude intervals. The Satellite Infrared Spectrometer (SIRS) algorithm, which has been developed for retrieving temperature profiles from Nimbus-4 observations, was then used in an attempt to retrieve the simulated soundings from the theoretical irradiances. The cross section was finally reconstructed utilizing the

the retrieved soundings. Their results indicated that an infrared sounder possessing good accuracy was very capable of obtaining temperature profiles which could be used to describe the thermal gradients beneath a jet streak. While the retrieved soundings lacked the vertical resolution characteristic of radiosonde observations, the capability of a satellite sounder to obtain temperature profiles at very short intervals (1° of latitude or even less) can partially compensate for the lack of vertical detail. In a sense there is a trade off between the excellent vertical detail in rawinsondes and the fine horizontal detail possible in a series of satellite soundings.

While Togstad and Horn's (1974) results were encouraging, they dealt only with simulated data which were assumed to have been obtained from a cloud free area. Since the presence of clouds restricts the number and quality of soundings based on infrared observations, the performance of an infrared instrument in the real atmosphere remains in question. In this study we report on the results obtained using actual infrared observations made by the Infrared Temperature Profile Radiometer (ITPR) flown aboard Nimbus-5. This instrument has a theoretical accuracy approaching that assumed by Togstad and Horn. The Nimbus-5 satellite also contains a microwave instrument (Nimbus-E Microwave Sounder, or NEMS) which is capable of sensing through clouds. The approach used here is similar to that used by Togstad and Horn. Isentropic cross sections based on the Nimbus-5 soundings were constructed through a February 10, 1973 jet streak. From them, estimates of the geostrophic and gradient wind components perpendicular to the cross section were calculated and compared with similar estimates computed from a cross section based on radiosonde temperature data and also with wind reports obtained from observed balloon displacements. Three sets of satellite derived data were used: (1) the ITPR alone, (2) the NEMS alone, and (3) an amalgamation of the ITPR and NEMS data. Before examining the results a short description of the Nimbus-5 sounders will be given.

2. The Nimbus-5 ITPR and NEMS Sounders

Nimbus-5 was launched on December 11, 1972 in a sun-synchronous orbit, inclined at an angle of 80° to the equator. The orbit was nearly

circular with an elevation of about 1100 km. The ITPR instrument measures infrared radiation in seven spectral intervals, four of which are in the 15 micron CO_2 band. Assuming that the distribution of absorbing gases is known and that the atmosphere is cloudless, radiation in a spectral interval near the center of an absorption band is emitted from high altitudes while that in the wings of the band is emitted from lower altitudes. Although the energy in any particular spectral interval arises from an 8 km layer, a series of observations enables the inversion of the radiative transfer equation to obtain an estimate of a vertically smooth temperature profile.

In areas of partial cloud cover, clear column radiances can be inferred from radiance observations. Measurements made simultaneously in two window regions (3.7 and 11μm) aid in defining clear column radiances. Because the two window channels respond equally to a uniform opaque surface but unequally to a non-uniform surface, cloudy and clear areas can be detected. The variation in the radiance in one window channel with respect to the other is used to extrapolate observations to equivalent values for cloudless conditions. With the establishment of the clear column radiance for the window region, the clear column for any of the sounding channels can be specified. The details of this procedure are given by Smith et al. (1975). Since the ITPR instrument has a field of view of only 30 km, clear columns can be obtained in areas of considerable cloud cover, although not in regions of solid overcast. This represents a considerable advance over the SIRS instrument which had a field of view of 225 km. While the ITPR was designed to scan left and right of the orbital track, most of the ITPR soundings are derived from only nadir data, since the scan mechanism malfunctioned early in its life.

The NEMS instrument, which was not designed to scan, measures thermal radiation in five regions of the microwave portion of the spectrum. The three channels in the 0.5 cm oxygen band are used to retrieve temperature profiles. The spatial resolution of about 200 km is considerably larger than that of the ITPR instrument; however, clouds have little effect on the microwave observations. In fact, the NEMS instrument is capable of sensing to the surface even through an overcast. Only the

presence of clouds with a large liquid water content, typically precipitating cells, causes any significant attenuation. Staelin et al. (1975) have noted that clouds have affected less tha 0.5 percent of the NEMS temperature profiles. See The Nimbus 5 User's Guide, 1972 for further descriptions of the ITPR and NEMS instruments.

Since a number of different temperature profiles could fit a given set of radiance measurements, some type of first guess profile is needed ao narrow the search for a solution. The Nimbus-5 temperature profiles are obtained from the radiances using a "minimum information" inverse solution of the radiative transfer equations. A large historical sample of radiosonde and rocketsonde profiles has been used to calculate corresponding theoretical radiances. These values have been employed by the National Environmental Satellite Service to calculate coefficients for the regression model from which the guess profile is obtained. See Smith et al., (1970).

In addition to the separate ITPR and NEMS soundings, a set of amalgamated soundings have been prepared by the Meteorological Satellite Laboratory of the National Environmental Satellite Service. The amalgamated sounding processing technique is centered about the ITPR data, with the NEMS data providing a supporting role where it overlaps with the ITPR measurements. See Smith et al. (1975). In this study cross sections based on each of the three sets of soundings have been prepared: (1) ITPR, sometimes referred to as Solution 1, (2) NEMS or Solution 2, and (3) amalgamated soundings (ITPR plus NEMS), called Solution 3. As noted in the introduction, the normal components of geostrophic and gradient winds derived from cross sections based on these three sets of data will be compared with winds derived from radiosonde thermal data and the rawin observations.

3. The Synoptic Case of 12 UT February 10, 1973.

Twenty-four hours before the time period chosen for this study, a trough at the 300 mb level and an associated jet streak were propagating across the Gulf of Mexico. At the surface, a cold front was located from the central Gulf through northern Florida. Rapid amplification of a frontal wave occurred as the jet approached the surface front. While the ensuing disturbance moved northeastward across central Florida, it

caused record snowfalls of 36-61 cm from central Alabama to North Carolina and severe thunderstorms in southern and central Florida. By 12 UT February 10, 1973 the intense cyclone was centered 300 km off the South Carolina coast. Fig. 1 portrays the surface, 500 and 300 mb charts. Superimposed upon the surface map is the 1634-1644 UT Nimbus-5 orbital path. A well-defined trough was present at both 500 and 300 mb with an indication of a closed center over southeastern Alabama. Strong temperature gradients over Florida at upper levels suggested that a pronounced jet streak was present above 300 mb. The 300 mb isotach analysis shows a 65 m sec^{-1} isotach area extending into central Florida. However, the wind data on the 300 mb chart was inadequate to accurately locate the isotach maximum of the jet streak, since only two of four Florida rawinsonde wind observations reached the 300 mb level.

4. Procedures

Rather than directly comparing the thermal gradients obtained at various levels from the three cross sections based on the Nimbus-5 solutions with those obtained from the radiosonde data, the derived wind fields normal to the cross sections will be employed. Essentially, a comparison of the thickness gradients along the cross sections will be made. One advantage of this approach is that the derived winds from both the satellite and radiosonde cross sections can be compared with the observed winds.

In computing estimates of the wind components normal to each cross section, isobaric layer mean temperatures were calculated at 2° latitude intervals along the cross section. The hypsometric equation was employed to compute equivalent thickness values. Gradients of these thickness values were then used to obtain the geostrophic shear. In all cases, the 850 mb geostrophic wind obtained from the 12 UT February 10 NMC analysis provided a base level wind. Thus, the normal component of the geostrophic wind was estimated using

$$u_{geo} = u_{geo,850} - \frac{g}{f} \frac{\Delta z}{\Delta n}, \qquad (1)$$

where u_{geo} is the normal component of the geostrophic wind, g is gravity, f is the Coriolis parameter, Δz is the geopotential thickness between

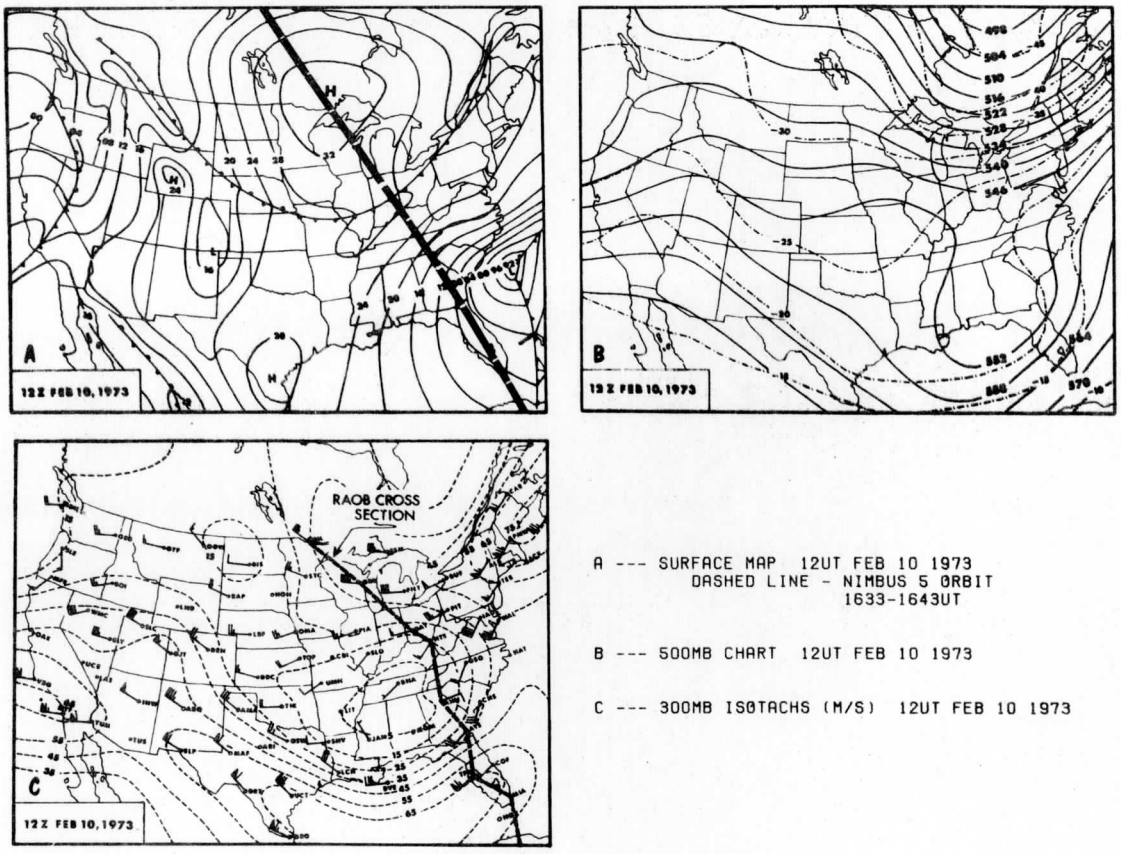

A --- SURFACE MAP 12UT FEB 10 1973
DASHED LINE - NIMBUS 5 ORBIT
1633-1643UT

B --- 500MB CHART 12UT FEB 10 1973

C --- 300MB ISOTACHS (M/S) 12UT FEB 10 1973

Fig. 1. Synoptic charts for 12 UT February 10, 1973.

two isobaric levels and Δn is, in this study, 2 degrees of latitude, the horizontal distance interval with which Togstad and Horn (1974) obtained their best results. For the first layer above 850 mb, a 150 mb pressure interval was used to obtain wind estimates for the 700 mb level. For subsequent layers, 100 mb pressure intervals were used up to the 100 mb level.

Estimates of the normal wind components obtained in the manner described above departed greatly from the observed winds in some portions of the cross sections. These departures will be discussed in the next section. Since significant cyclonic curvature was present in this February 10, 1973 case, the wind estimates were refined employing the gradient wind correction.. This was accomplished using the gradient wind expression in the form:

$$K_H u^2_{gr} + f u_{gr} - f u_{geo} = 0 , \qquad (2)$$

where K_H is the horizontal trajectory curvature, u_{geo} is the geostrophic normal wind component, and u_{gr} is the gradient normal wind component. Each of the computed geostrophic components, including normal components of the 850 mb geostrophic wind, were substituted into (2) which was solved quadratically to obtain the normal components of the gradient wind. To simplify the procedure, contour rather than trajectory curvatures were utilized. Since an examination of the upper air charts for the 12 UT February 10, 1973 and 00 UT February 11, 1973 times showed that the cyclone was in a mature stage and that the contour patterns at the major levels (850, 700, 500, 300, and 200 mb) were changing only slowly with time, the assumption that the contours approximate the trajectories appears not to have been seriously violated.

5. Results

In Fig. 2 are shown the isentropic cross sections constructed from the 12 UT February 10, 1973 radiosonde data and the 1630 UT Nimbus-5 soundings. As shown in Fig. 1, the radiosonde cross section does not exactly coincide with the Nimbus-5 orbit. The time difference of more than four hours also places some limitations on comparisons of the radiosonde and satellite data; however, since the synoptic pattern was only slowly evolving with time, this deterrent is not great. All cross

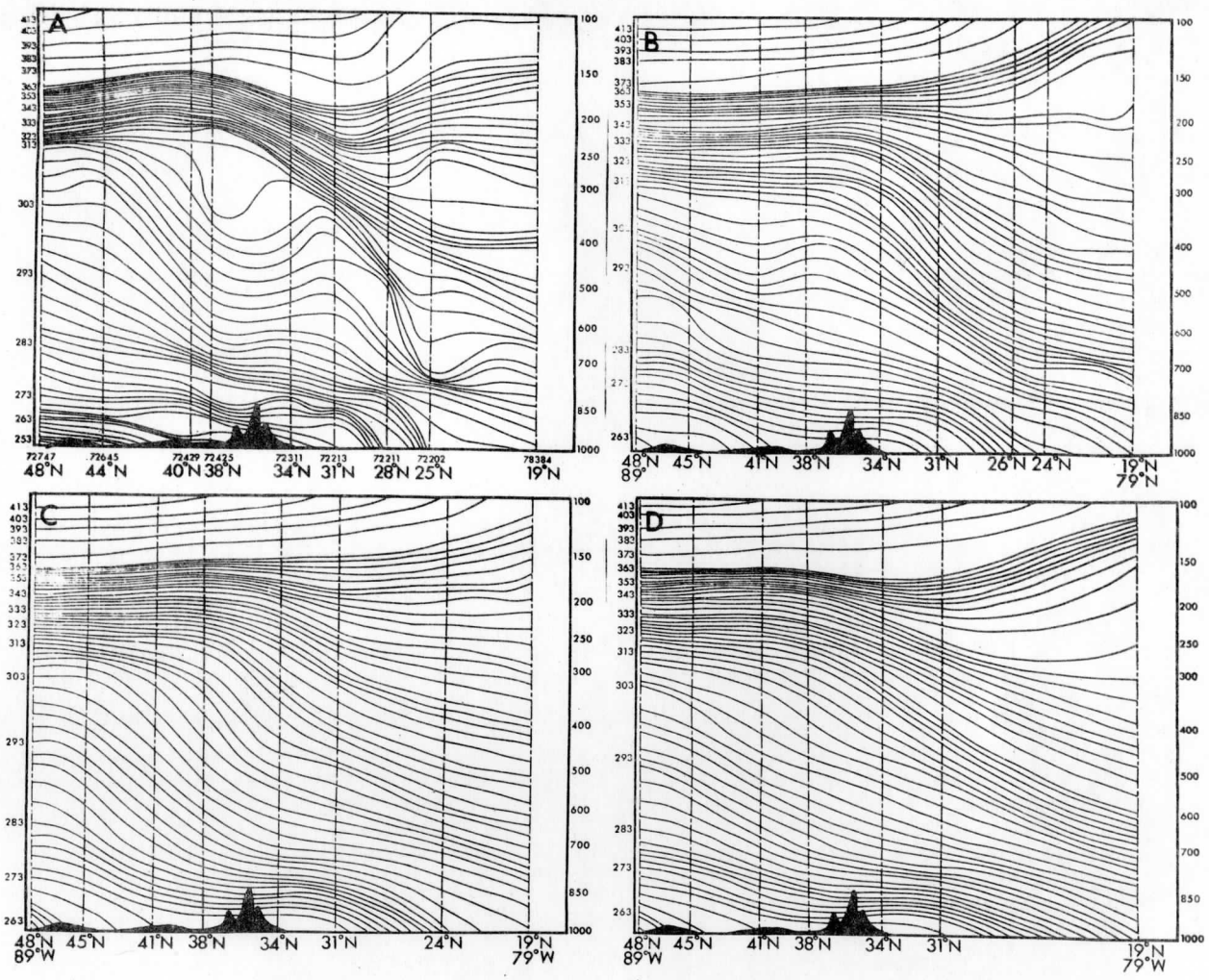

ISENTROPIC CROSS SECTIONS (2K INTERVAL, EXCEPT 10K ABOVE 363K)

A. RAOB - 12UT FEB 10 1973
(INTERNATIONAL FALLS - GRAND CAYMAN)

B. NIMBUS 5, ITPR 1633-1643UT

C. SAME AS B EXCEPT NEMS

D. SAME AS B EXCEPT ITPR+NEMS

Fig. 2. Isentropic cross sections (2K interval, except 10K above 363K). A) Radiosonde cross sections for 12 UT February 10, 1973, B) Nimbus-5 ITPR 1633-1643 UT February 10, 1973, C) Same as B except NEMS D) Same as B except ITPR and NEMS.

section analyses were done subjectively using the general analysis rules developed over the past few decades.

The most obvious feature of the comparisons displayed in Fig. 2 is the greater detail revealed by the radiosonde cross section. Although all four of the cross sections show pronounced baroclinity between 34 and 24N, the radiosonde cross section concentrates the baroclinity in several limited areas. Of the three sets of Nimbus-5 soundings, the ITPR data provide the greatest detail, with the NEMS data producing a considerably smoother field. Since the NEMS instrument has a field of view almost seven times that of the ITPR instrument, this smoothing should be expected. In addition, the existence of fewer sensing channels in the NEMS instrument reduces the vertical resolution. However, it should be remembered that while the ITPR needs some breaks in an overcast to produce a sounding to the surface, the microwave scanner is capable of making observations through an overcast. The solution 3 data (ITPR plus NEMS) produce a pattern which is somewhat smoother than the ITPR but more detailed than the NEMS cross section. Unfortunately, since no amalgamated soundings were available between 31 and 19N conclusions regarding the solution 3 results are somewhat restricted.

The thickness gradients obtained from the four cross sections were evaluated over 2° latitude intervals to obtain the geostrophic shear in the isobaric layers noted previously. Since the mean temperature in each of these layers was used to obtain the thickness value, the effect of the greater vertical detail provided by the radiosonde is partially obscured. The geostrophic shear values were combined with the 850 mb geostrophic wind (from the NMC analysis) to obtain the normal components of the geostrophic wind shown in panels B, C, D, and E of Fig. 3.

In panel A, the isotachs of the normal component of the observed winds clearly reveal a jet core exceeding 60 m s^{-1} centered near 270 mb at 28N. To the north of the jet, a rather deep layer of easterly geostrophic wind components is found, with values of -10 m s^{-1} reaching to the 300 mb level. While the general pattern of the geostrophic components derived from the radiosonde and satellite sounding temperature data is quite similar to the observed winds, the magnitudes of the wind

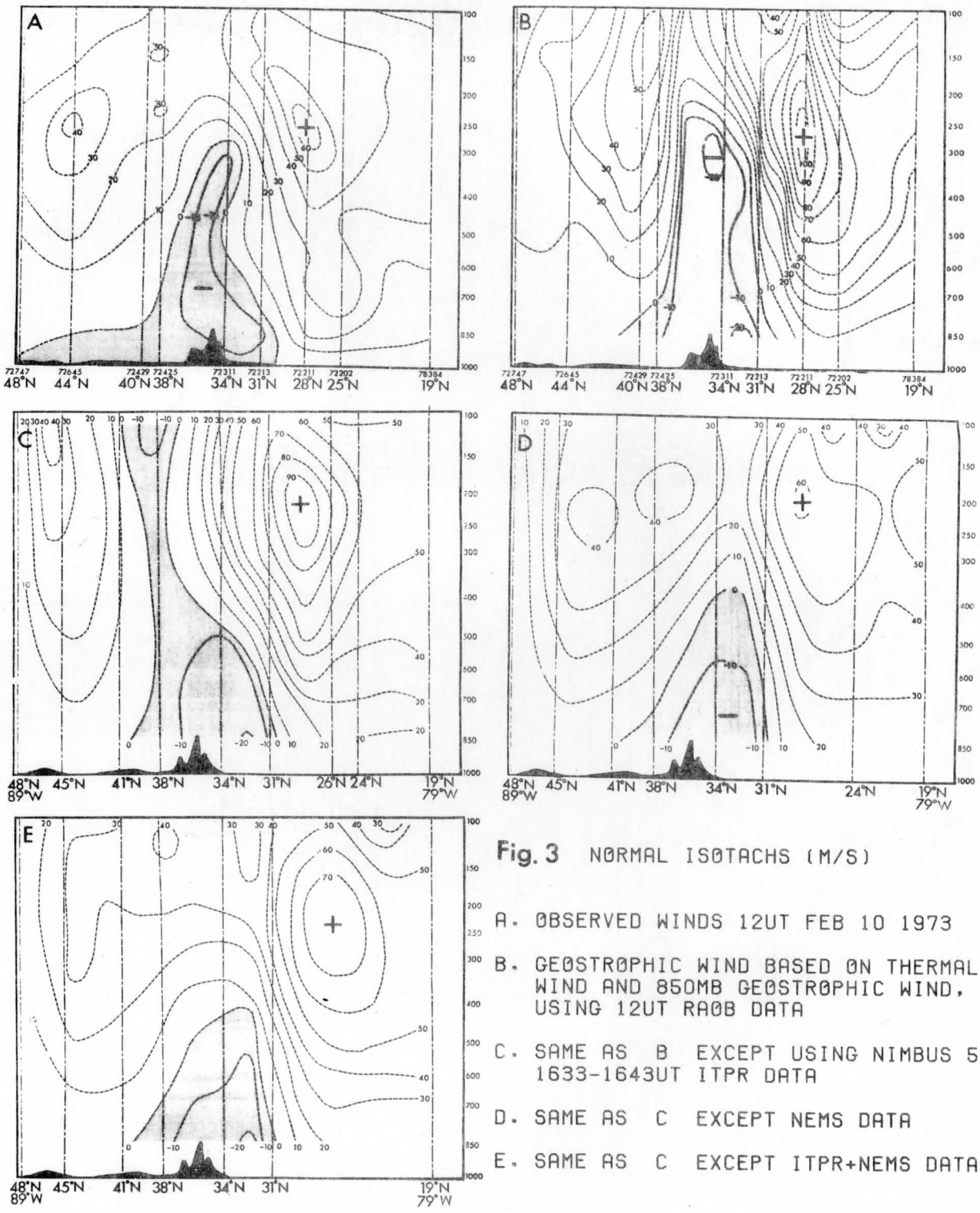

Fig. 3 NORMAL ISOTACHS (M/S)

A. OBSERVED WINDS 12UT FEB 10 1973

B. GEOSTROPHIC WIND BASED ON THERMAL WIND AND 850MB GEOSTROPHIC WIND, USING 12UT RAOB DATA

C. SAME AS B EXCEPT USING NIMBUS 5 1633-1643UT ITPR DATA

D. SAME AS C EXCEPT NEMS DATA

E. SAME AS C EXCEPT ITPR+NEMS DATA

maxima differ considerably. The most obvious difference is in the strength of the jet core. Although both the radiosonde and ITPR derived geostrophic winds (normal components) place the wind maxima at 28N, the radiosonde maximum is 109 m s^{-1} and the ITPR maximum is 99 m s^{-1}, compared to an observed absolute maximum of 70 m s^{-1}. Because of the poorer resolution provided by the NEMS data, the wind maxima is only 63 m s^{-1}. The merged, Solution 3 results produce an intermediate value of 80 m s^{-1}.

Because of the excessive wind speeds obtained in deriving the geostrophic wind components from the thermal data, the gradient thermal wind relationship (Equation 2) was employed to calculate the wind components normal to the cross sections. At 850, 700, 500, 300, and 200 mb, the curvature (K_H) was obtained from the NMC height analyses. At intermediate levels, such as 600 mb, the curvature values were interpolated linearly. Since the jet was located in a region of rather pronounced cyclonic curvature, the gradient wind speeds were significantly less than the geostrophic values.

Cross sections of the normal components of the gradient winds are shown in Fig. 4. The panel arrangement is the same as in Fig. 3 with the normal components of the observed winds repeated from Fig. 3A. Panel B displays the gradient wind components derived from the radiosonde thermal data, while panels C, D, and E show the results obtained from the Nimbus-5 solutions 1, 2, and 3, respectively. Although the patterns of the geostrophic and gradient wind isotachs for the respective cross section in Figs. 3 and 4 are essentially the same, the magnitudes of the values differ considerably. For example, in the jet core the maximum gradient wind speeds calculated from the radiosonde thermal data and ITPR data are 69 and 68 m s^{-1} respectively, versus geostrophic values of 109 and 99 m s^{-1}.

In comparing the radiosonde derived gradient winds (panel B) with the observed winds (panel A), good agreement is found in the region of the jet core over Florida; however, the easterly gradient wind components centered near 36N are stronger than the observed values (-20 m s^{-1} versus -10 m s^{-1}). To the north, an observed westerly wind maximum is located at 44N and 250 mb, which is poleward of the gradient wind maximum calculated from the radiosonde thermal gradients.

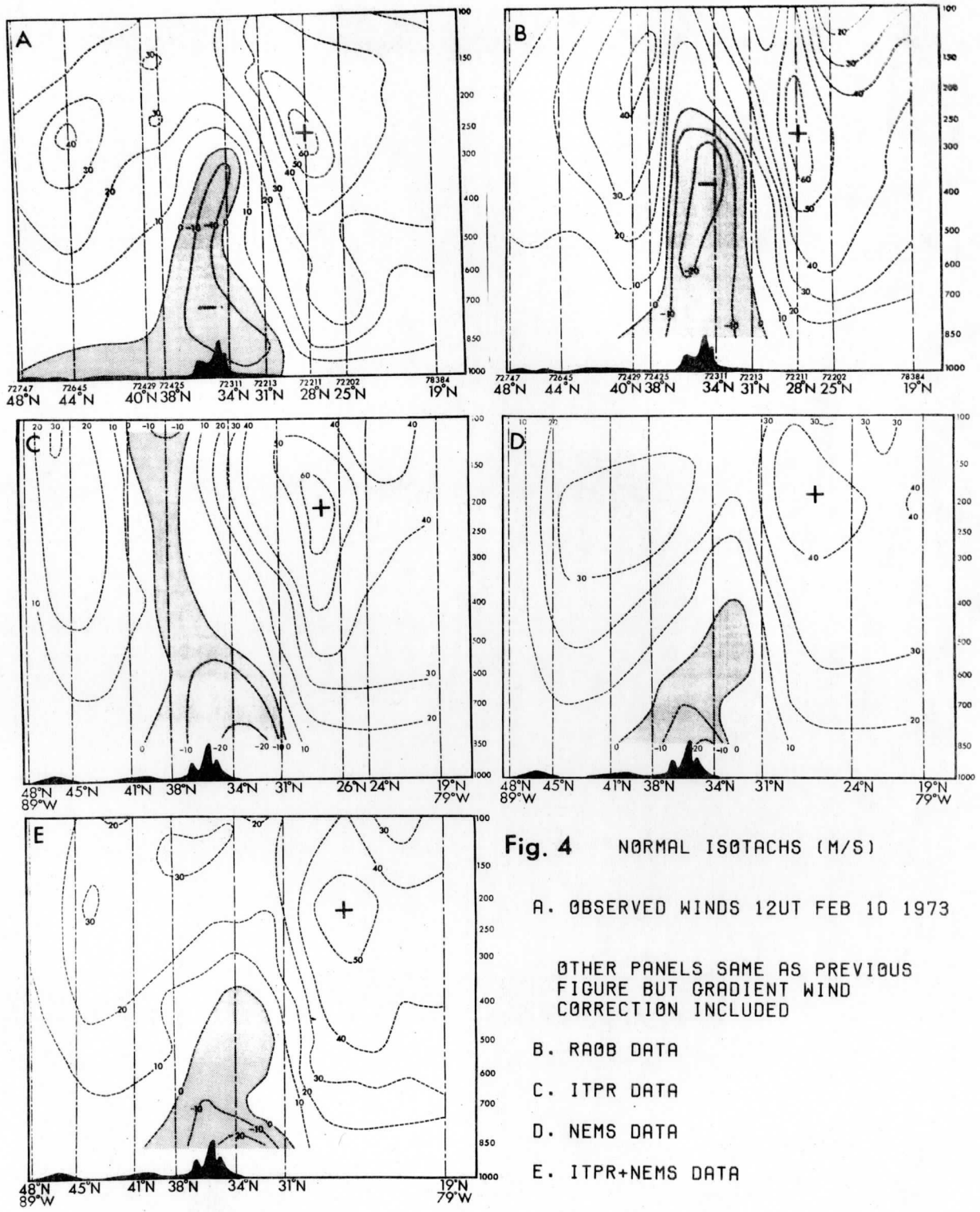

Fig. 4 NORMAL ISOTACHS (M/S)

A. OBSERVED WINDS 12UT FEB 10 1973

OTHER PANELS SAME AS PREVIOUS FIGURE BUT GRADIENT WIND CORRECTION INCLUDED

B. RAOB DATA

C. ITPR DATA

D. NEMS DATA

E. ITPR+NEMS DATA

The gradient winds derived from the ITPR data (panel C) are in general agreement with those derived from the radiosonde data (panel B) in the region south of about 36N. However, north of this latitude there are some significant differences. In the ITPR data, the region of easterly winds reaches above 100 mb, while in the radiosonde data the easterlies terminate at about 250 mb. This is typical of the smoothing often found near the tropopause in satellite soundings. The band of easterly winds in the ITPR cross section also leans toward the north with increasing altitude, extending as far north as 40N. This contrasts with the strong westerlies found in this region in panel B and with the observed moderate westerlies (panel A). Panels D and E, which display the results obtained from the NEMS and solution 3 data, show better agreement with both the radiosonde derived and observed winds in the region north of 36N. The easterlies extend only to 400 mb with moderately strong westerlies in the 200-100 mb layer at 38-40N. A possible explanation of the improvement provided by the NEMS data lies in the pattern of cloudiness in this region. While numerous breaks were present in the cloud cover over the southern portion of the cross section, the heavier overcast conditions in the region from 36 to 40N may have led to cloud contamination in the ITPR soundings north of the jet core, even though the soundings passed the NESS program check for cloud contamination.

In the region of the jet core itself the gradient winds obtained from the ITPR data are very close to those of the observed winds. In fact, there appears to be greater agreement between the values derived from the ITPR and the observed winds in this region than between the gradient wind components derived from the radiosonde and the observed winds. Part of the improvement in the ITPR data here may have resulted from the inclusion of additional partial soundings in the analysis, some as close as 55 km to the complete soundings. The partial sounding data were produced in areas where the ITPR instrument was unable to produce a full sounding, usually because of cloud contamination.

In Fig. 5 are summarized the comparisons between the gradient wind estimates obtained from the various Nimbus-5 soundings and two sets of conventional wind data: the gradient winds derived from the radiosonde thermal data and also the rawin wind observations. Part A of the figure

Figure 5
--- COMPARISONS ---

A. RMS DIFFERENCES (M/S) OF ISOTACH FIELDS DERIVED FROM THERMAL GRADIENTS. GRADIENT WIND CORRECTION INCLUDED

STANDARD -- WINDS DERIVED FROM RAOB THERMAL GRADIENTS

LATITUDE RANGE	RAOB	ITPR	NEMS	ITPR+NEMS
48 - 20N	0.0	14.2	11.3	10.2
32 - 24N	0.0	10.5	11.9	11.0

STANDARD -- OBSERVED WINDS

LATITUDE RANGE	RAOB	ITPR	NEMS	ITPR+NEMS
48 - 20N	10.2	9.3	9.4	7.7
32 - 24N	10.3	8.4	10.5	9.5

B. FEATURES OF JET CORE

	OBSERVED	RAOB	ITPR	NEMS	ITPR+NEMS
LATITUDE (N)	28	28	28	28	26
ALTITUDE (MB)	270	270	200	200	225
SPEED (M/S)	70	69	68	48	57

expresses the comparisons in terms of the Root Mean Squares (RMS) differences. In one case, the gradient wind values derived from the radiosonde data were used as a standard, and in the other, the observed (rawin) winds were chosen as a standard. The RMS differences, computed at 2° latitude intervals for the 850, 700, 600, 500, 400, 300, and 200 mb levels, were calculated both for the entire cross section (48-20N) and separately for the limited region of the jet core (32-24N). For the entire cross section, the smallest RMS differences (10.2 m s^{-1}) are between the solution 3 and radiosonde results, while the largest differences are between the ITPR and radiosonde data (14.2 m s^{-1}). The large differences are probably due to the poor comparison between the ITPR and radiosonde results between 36 and 42N, since in the region of the jet core, the ITPR results show the smallest RMS differences.

Using the observed winds as a standard, the gradient winds calculated from Nimbus-5 sounding data almost consistently produced smaller RMS differences than the winds derived from the radiosonde data. In the jet core region, the ITPR soundings led to an RMS difference of only 8.4 m s^{-1} compared with 10.3 m s^{-1} for the radiosonde data. The larger value (10.5 m s^{-1}) for the NEMS results is likely due to the poorer resolution provided by this instrument. Recall that it has a field of view of 200 km and senses in only three spectral intervals.

Although RMS differences provide some measure of the performance of the Nimbus-5 sounders, some important features of the derived wind fields are obscured in the statistics. The poorer showing of the ITPR soundings in the region between 36 and 42N has already been noted. Perhaps of greater importance is the ability of the various sounding systems to locate the position of the jet core. Some comparisons are shown in part B of Fig. 5. The fact that the observed winds and the gradient wind components derived from the radiosonde, ITPR and NEMS all place the jet core at 28N is impressive. The solution 3 results, which place the jet at 26N, are probably due to the lack of any amalgamated soundings between 31 and 19N. A comparison of the maximum speeds obtained from the rawin reports with those derived from the radiosonde and ITPR data is equally impressive. The importance of using the gradient thermal wind relationship in regions of curved flow should again be emphasized.

The weaker wind maximum obtained from the NEMS data is undoubtedly related to its large field of view, which leads to poor resolution in strong baroclinic zones.

Vertically, the observed winds and radiosonde derived gradient wind components place the altitude of the jet core at 270 mb, compared with 200 mb for the ITPR and NEMS data and 225 mb for the solution 3 case. The failure of the satellite soundings to better resolve the altitude of the maximum winds is likely due to the poor vertical resolution provided by satellite soundings compared to that available in radiosonde observations. However, it should also be noted that the radiosonde cross section thermal analysis was biased by the observed winds, since their shear was used to aid in determining the slope of the isentropes at the radiosonde stations. Since observed winds do not accompany satellite soundings, this strong point of isentropic cross section analysis could not be applied to the satellite cases.

As noted earlier, all of the soundings were analyzed subjectively by Kapela, with some assistance from Horn. Since both Kapela and Horn were familiar with the case, another experienced analyst (Bromwich, 1975), who was completely unfamiliar with the case, repeated the cross section analyses, paying particularly attention to the region of the jet core. His results led to a position of the jet maximum which was less than 1° latitude from that obtained by Kapela and Horn.

6. Conclusions

The results obtained in this real atmosphere case tend, for the most part, to confirm the conclusion of Togstad and Horn (1974) that satellite soundings of the quality of Nimbus-5 are capable of reasonably describing the thermal gradients beneath a jet streak. Even though considerable cloud cover was present in this February 10, 1973 case, the small field of view of the ITPR and the cloud penetrating capability of the NEMS instrument led to positions of the jet core which had identical latitudes to those obtained from the observed winds and radiosonde derived gradient winds. The maximum winds obtained from the rawin data, radiosonde soundings and ITPR soundings are within 2 m s^{-1} of each other. In a relatively broad band north of the jet core the ITPR soundings failed to adequately describe the wind field,

probably because of some cloud contamination in the infrared measurements; however, in this region the NEMS soundings produced quite reasonable results.

In comparing the normal wind components obtained from the satellite data with the observed winds, smaller RMS differences are achieved than between the radiosonde derived winds and the observed winds. Thus, it appears that infrared sounders of the quality of the Nimbus-5 ITPR combined with a microwave sounder with a small field of view should provide soundings which can be used to locate the jet stream and the jet streaks which propagate along it.

Finally, it should be reiterated that the gradient thermal wind relationship provides a much better estimate of the observed wind field in regions of curved flow.

7. Acknowledgments

The authors wish to thank Dr. William L. Smith of NESS for providing the Nimbus-5 soundings, David Floyd for assisting in plotting the cross sections, Scott Singer for aiding in the computer programming, and Dr. Ralph Petersen in revising the manuscript. Special thanks are extended to David Bromwich for independently analyzing some of the cross sections. The research was supported by the National Environmental Satellite Service of NOAA under Grant 04-4-158-2.

References

Bromwich, David, 1975: Personal Communication, University of Wisconsin-Madison, Department of Meteorology.

Cahir, J.J., 1971: Implications of circulations in the vicinity of jet streaks at subsynoptic scales. Ph.D. thesis, The Pennsylvania State University, 170 pp.

Danielson, E.F., 1959: The laminar structure of the atmosphere and its relation to the concept of the tropopause. Arch. Meteor. Geophys, Bioklim., A, 11, 293-332.

Duquet, R.T., E.F. Danielson and N.R. Phares, 1966: Objective cross section analysis. J. Appl. Meteor., 5, 233-245.

Newton, C.W., 1954: Frontogenesis and frontolysis as a three-dimensional process. J. Meteor., 11, 449-461.

Nimbus-5 Users Guide, 1972: Goddard Space Flight Center, Greenbelt, Md.

Smith, W.L., H.M. Woolf and W.C. Jacob, 1970: A regression method for obtaining real-time temperature and geopotential height profiles from satellite spectrometer measurements. Mon. Wea. Rev., 98, 582-603.

Smith, W.L., H.M. Woolf, C.M. Hayden and W.C. Shen, 1975: Nimbus-5 Sounding Data Processing System Part II: Results, Final Report, NASA Contract S-70244-AG.

Togstad, W.E. and L.H. Horn 1974: An application of the satellite indirect sounding technique in describing the hyperbaroclinic zone of a jet streak. J. Appl. Meteor., 13, 264-276.

Objective Cross Section Analysis Incorporating Thermal Enhancement of the Observed Winds

Thomas M. Whittaker and Ralph A. Petersen
Department of Meteorology, University of Wisconsin-Madison, Madison 53706

Abstract

Overlapping second order Lagrangian polynomials are used to construct analyses of cross sectional thermal fields defined by upper air sounding observations. Estimates of geostrophic winds are obtained from the thermal wind relationship. Thermal wind information is also combined with normal components of the observed wind to obtain a thermally enhanced observed wind analysis. Comparison of results using the techniques shown are presented and compared with a previous objective analysis technique. Examination of the results indicates the applicability of the technique both for operational and research purposes.

1. Introduction

For years, atmospheric cross sections have provided the synoptic meteorologist with an alternative perspective from which to view the atmosphere. Using the relatively rich vertical arrays of data available from a given set of radiosonde observations, more detailed information regarding the distributions of atmospheric thermal and velocity fields and their interrelationships can be obtained from cross sectional analyses than from conventional quasi-horizontal analyses alone. In addition, the synthesis of several cross sections with conventional map analyses provides a degree of vertical continuity which otherwise could not be achieved.

Historically, many important discoveries regarding the structure of fronts and cyclones and their relation to the jet stream have been made using subjectively analyzed cross sections. See Danielsen (1959) and Newton (1954). Unfortunately, cross sections constructed and analyzed by hand have seldom been utilized in real time situations, having been restricted primarily for research purposes. As detailed by Shapiro and Hastings (1973), the laborious process of obtaining a hand analyzed cross section introduces a deterrent to their extended use. Yet another drawback is the subjectivity of the analyses. Not only are there inconsistencies between individual analyses, but theoretical constraints can be only qualitatively integrated into the subjective analysis of the normal wind component.

Two previous attempts have been made to produce objective (computer generated) cross sectional analyses. The first, by Duquet et al. (1966), proved unsuccessful, primarily due to its inability to adequately resolve the baroclinic structure of the atmosphere. The method developed by Shapiro and Hastings met the constraints of cross sectional analysis using Hermite polynomials to successfully describe the vertical two-dimensional thermal structure of the atmosphere. However, the technique did not attempt to incorporate consistency between the analyses of the thermal field and the observed wind field.

In this article, a method is presented which not only speeds the

thermal analysis, but also integrates dynamical information derived from the thermal field into the analysis of the observed wind. Through such a technique, for example, more detailed and thermally consistent investigations of the jet stream and its relation to the extratropical cyclone might be undertaken using both conventional radiosonde data and the voluminous amount of data that may soon be made available from satellite observations.

2. Objective analysis technique

a. Thermal field

As in the case of subjective analysis, several goals were prescribed for the objective analysis technique. The original data field must be preserved at all reporting levels at each station. Vertical data interpolation is done linearly with respect to p^{κ} in regions between reporting levels. The isentropes should maintain a smooth continuous character over the entire cross section, and must not violate the static stability criterion that $\frac{\partial p}{\partial \theta} < 0$, where p is pressure and θ potential temperature. Finally, the technique should maintain simplicity to aid in its implementation and to minimize the amount of computer time necessary to perform the analysis.

In order to describe the position of an isentrope between any two of the n number of stations in a particular cross section, n-2 second-order Lagrangian polynomials (Greenspan, 1970) of the form

$$y = \sum_{i=m}^{m+2} y_i L_i \quad ; \qquad L_i = \frac{\prod_{j=m}^{m+2} (x_j - x)}{\prod_{j=m \; j \neq i}^{m+2} (x_j - x_i)} \qquad 1 \leq m \leq n-2$$

are calculated and combined linearly to obtain smooth isentropes in a manner similar to that described by Bleck and Haagenson (1968). Using four unevenly spaced successive data points (A, B, C and D) as shown in Fig. 1a, two second-order polynomials are fit to the data sets A-B-C (dashed) and B-C-D (dotted). In the intervening region between points B and C the two polynomials are merged using linear weighting dependent upon the distance from the points. The resulting polynomial (solid line) connects the points as smoothly as does a third-order

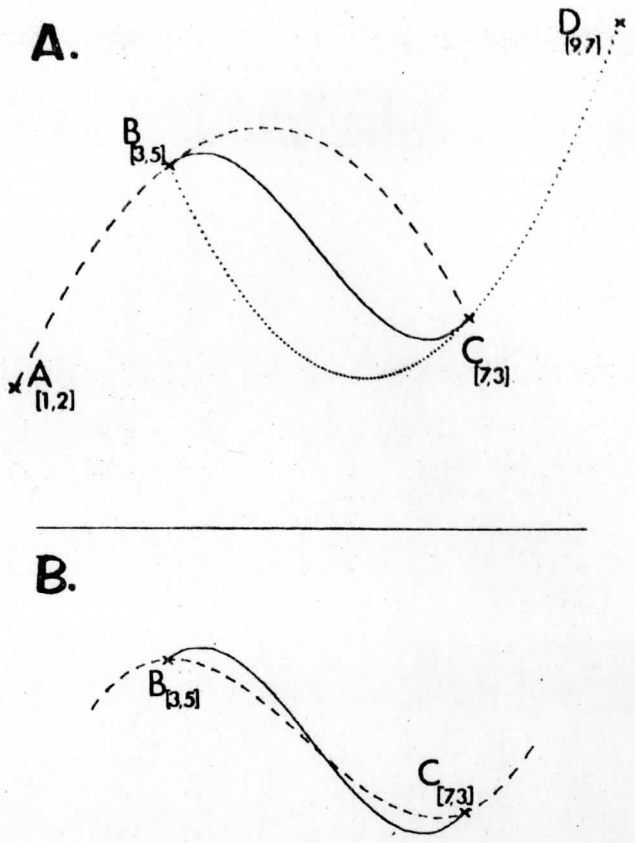

Fig. 1. Illustration of overlapping polynomials. (A) Two quadratic Lagrangian polynomials connecting points A, B and C (dashed) and points B, C and D (dotted). (The x, y coordinates of the points are shown in brackets.) Linear merger of the two polynomials between B and C shown by solid line. (B) Comparison of linearly merged result from Fig. 1a (solid) with third order polynomial fit to all four points, A, B, C and D (dashed).

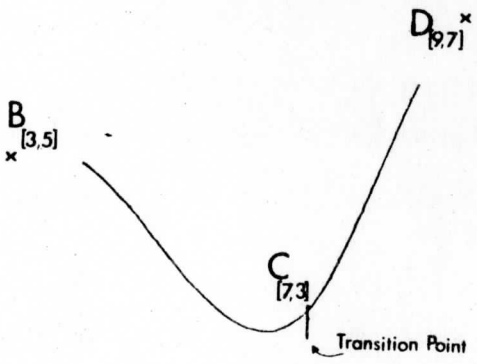

Fig. 2. Illustration of the smooth transition, at data point C, between two overlapped quadratic Lagrangian polynomials.

polynomial connecting all four points (dashed line in Fig. 1b). Additionally, the linear merger of the set of polynomials dictates smooth transitions at the data points as shown in Fig. 2, without the need for computing a derivative of the polynomials at the points of transitions as was the case using Shapiro and Hastings (1973) technique involving third-order Hermite polynomials.

To lessen the amount of computer time required, most computations are made in x-y plotter coordinates, rather than working directly with pressure as the vertical axis. At each station, values of pressure at the reporting levels are converted to vertical (y) plotter coordinates scaled by p^K. The locations of the isentropes are calculated at each station using linear vertical interpolation in these x-y plotter coordinates. This achieves the same result as linear interpolation with p^K in pressure coordinates. The horizontal (x) spacing between stations is computed using spherical trigonometric relationships and the latitude and longitude of the stations (Appendix A). The isentropes, computed at 2K intervals, are then drawn at a specified interval directly onto the analysis starting at the lower surface and working upward using the method of overlapping polynomials described above. In regions where the polynomials produce superadiabatic layers, enough mass is extracted from the layer above to defeat the superadiabatic condition by at least one plotter increment, while maintaining the total mass within successive 20K isentropic layers.

Not all isentropes drawn on a cross section can be followed continuously from one side to the other, since inevitably some isentropes intersect either the upper or lower boundary of the cross section. Where this occurs, station data are by necessity extrapolated linearly upward and downward, allowing the polynomials to extend through the boundaries. The following criteria are observed:

In regions underground, $\frac{\partial p}{\partial \theta}$ is defined as $\frac{(p_{\theta_k} - p_{\theta_s})}{(\theta_k - \theta_s)}$

where p is the pressure, θ_k is the first isentrope above the ground, and θ_s is the surface potential temperature. Further limits are specified such that $\frac{\partial p}{\partial \theta}$ must be within the range

from -20.0 mb K^{-1} to -100.0 mb K^{-1}. These conditions allow isentropes to extend into the ground while limiting the influences of low level diurnal effects, which do not necessarily represent atmospheric conditions in regions other than that directly above the surface at the reporting station.

Aloft, if a station terminates more than 150 plotter units (typically 3.8 cm) from the top of the cross section, the region above is analyzed as if the station were not present, thus allowing the inclusion of partial soundings. Otherwise, the vertical distance between the last two reported isentropes is extrapolated upward.

Using the techniques given above, a complete description of the thermal field can be achieved numerically. Only between the two outermost stations might the objective analysis differ greatly from a subjective one, since overlapping of polynomials cannot be used in these regions. However, it is possible to eliminate this problem by adding supplementary soundings outside the regionsof main interest.

b. Wind Field

In any cross sectional analysis, it is desirable to obtain a wind field which is vertically and horizontally consistent with the derived thermal field. To accomplish this, values of potential temperature are linearly interpolated to a 40 by 40 grid, which is evenly spaced in the x-p^{K} cross sectional analysis area, during the computation of the isentropes. Once the thermal field has been completely defined, the gridded values of potential temperature are used to compute values of the geostrophic wind shear [1] using

$$u_g = \frac{R_d}{f} \frac{\Delta T}{\Delta x} \ln \frac{p_L}{p_u} ,$$

where u_g is the geostrophic shear between any two pressure levels

[1] In this article, shear is used to refer to the difference between the value of the geostrophic wind normal to the cross sectional plane at any level and the value at a particular reference level.

p_L (lower) and p_u (upper), R_d the gas constant, f the coriolis parameter, T the temperature and x the distance along the cross section from left to right. The vertical integration is normally initialized at the first grid level at least 100 mb above the ground. This level has been chosen to avoid the influence of the ageostrophic motions at low levels.

If the components of the geostrophic velocity normal to the cross section at any specified level are given, these values can be combined with the geostrophic shear to obtain estimates of the normal components of the geostrophic wind. Similarly, information about the radii of curvature (obtained from upper level charts) along the cross section can be utilized to estimate the gradient wind.

The most important difference between this and previous objective cross sectional analysis routines is the technique applied to the normal component of the observed wind. A method has been developed which combines information obtained from the thermal field with the reports of the observed wind to enhance the wind field both between stations and between reporting levels at each station.

The geostrophic shear is first calculated for the 40 by 40 grid describing the area of the cross section. These values are then interpolated to each of the reporting levels at the stations. At each level, a measure of the ageostrophic component of the wind is calculated as the difference between the observed wind and geostrophic shear. The resulting values are interpolated back to the 40 by 40 grid and added to the shear field to arrive at a representation of the observed wind field. This field not only maintains the normal components of the observed wind at each station's reporting levels but also includes a thermal-dynamic consistency elsewhere, obtained from the thermal wind relationship. Thus an analysis of the observed wind is enhanced and usually made more representative of the actual wind field than is either the derived field of geostrophic wind or a simple independent analysis of the observed winds.

3. Results

To illustrate the results obtained using the technique described here, we have chosen a 12UT December 7, 1963 cross section extending from Oakland to Peoria. This same cross section was objectively analyzed by Shapiro and Hastings (1973). No comparison between our objective analysis technique and subjective analyses are given here, as a comparison was already provided by Shapiro and Hastings. It was felt that a comparison of the two objective techniques would provide greater insight. The data used was obtained by manual extraction from the Northern Hemispheric Data Tabulations of upper air information. The following illustration is representative of the many cross sectional analyses accomplished using this technique.

Figure 3a duplicates the objective analysis of potential temperature and normal geostrophic wind component at 12UT December 7, 1963 originally shown in Shapiro and Hastings. Figure 3b illustrates an analysis of the same parameters using the technique described here. A comparison of these two figures shows general agreement between the two analyses, with upper frontal zones extending both to the west and east above the dome of cold air located near the center of the analysis. The geostrophic wind maxima are located at the same positions and are of approximately the same magnitudes. A closer examination of the figures shows small differences at the reporting stations. Figure 4 shows a tabulation of reported potential temperatures and isentropic intersections at several stations as computed in these two cross sections. The vertical data interpolation restriction appears to be more exactly followed by the technique described here. For example, the 284K isentrope shown in panel A is found between reports of 285.3K and 287.0K at Rapid City and at 286.1K at Lander. Similarly, the 280K isentrope intersects the North Platte sounding at 800 mb while the lowest reported potential temperature was 280.9K. The results from panel B, however, more accurately represent all of the data observed at these stations. These small difference aside, the overall picture obtained from these two analyses shows only minor discrepancies.

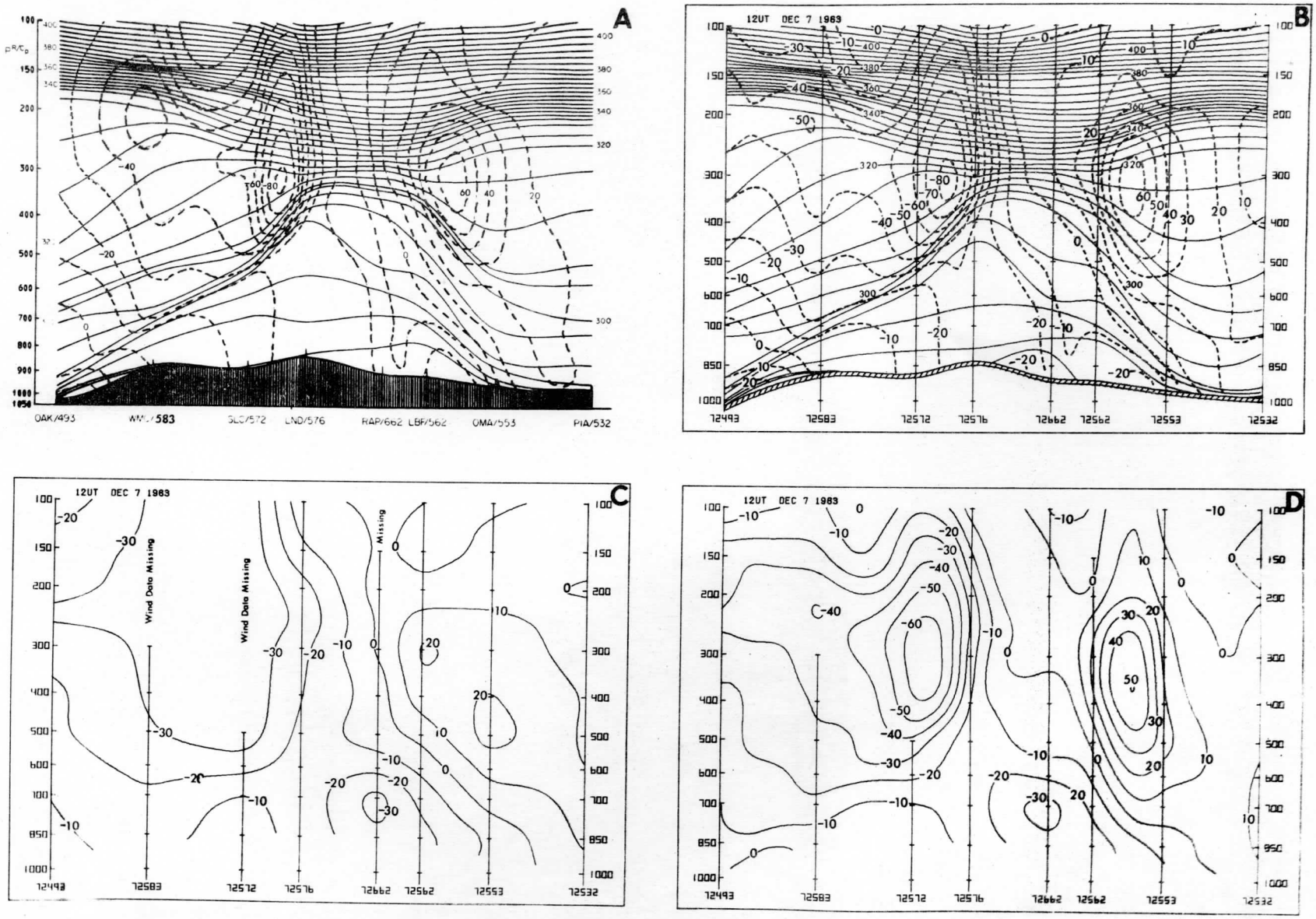

Fig. 3. Cross section for 12UT December 7, 1963 from Oakland (72493) to Peoria (72532), with intermediate stations Winnemucca (72583), Salt Lake City (72572), Lander (72576), Rapid City (72662), North Platte (72562) and Omaha (72553). (A) Duplicate of figure shown by Shapiro and Hastings (1973); isentropes (solid) at 4K intervals; normal component of geostrophic wind (dashed) in m s^{-1}. (B) Analyses of same data as (A), but using analysis method presented in this article. (C) Scalar analysis of normal component of observed wind as reported at manditory levels of stations (m s^{-1}). (D) Analysis of same data as (C), but using thermal enhancement technique.

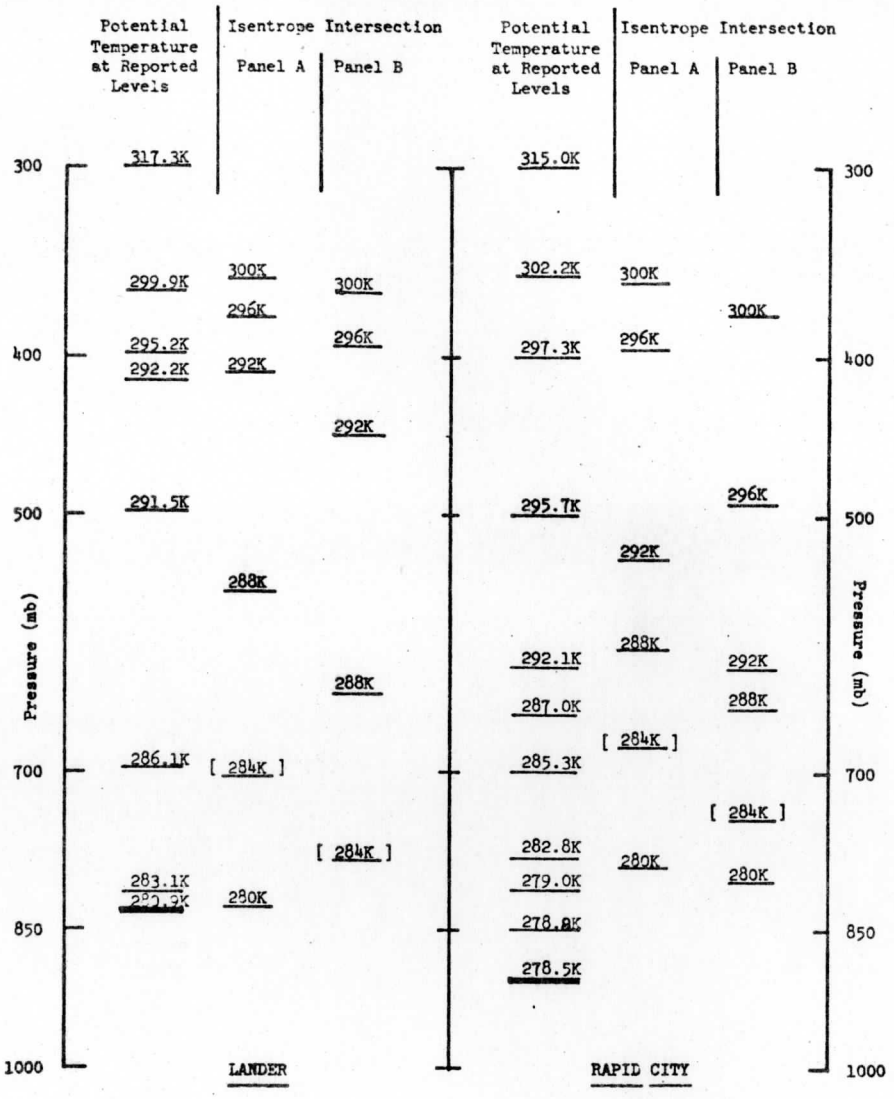

Fig. 4. Comparison of isentrope positions at Lander (72576) and Rapid City (72662) from analyses by Shapiro and Hastings (Fig. 3a), with those from the method presented in this article (Fig. 3b). For each station, the left column lists potential temperature as reported at all levels given in the Northern Hemisphere Data Tabulations, the center column shows isentrope location at the station as analyzed in Fig. 3a, and the right column shows those from Fig. 3b.

As stated previously, an important addition to our analysis technique is the incorporation of thermal-dynamic constraints into the analysis of the observed wind field. Figure 3c illustrates a scalar analysis of the normal component of the mandatory level winds as observed at the stations. Note that the wind reports terminated prematurely at Winnemucca, Salt Lake City and Rapid City. Three features of the analysis should be observed. First, the analysis is incomplete in the regions of missing data. Second, the two thermally supported maxima of the normal geostrophic wind component previously found between reporting stations are ill defined by the scalar analysis of the observed winds. Third, the low level northerly jet located at 700 mb above Rapid City was not found in the geostrophic wind field. Panel D, however, represents the merger of the station wind observations with the thermally prescribed field of geostrophic shear. The most striking feature is the reappearance of the jet cores located between stations near 300 mb, above the two upper frontal zones. It should be noted that the analysis conforms with the reported wind values, and that the maxima observed in these two cores are less than the geostrophic speeds shown in panel B. This is consistent with the subgeostrophic speeds normally found in regions of cyclonic curvature. The examples noted above demonstrate the capability of the thermal enhancement to approximate the wind field in regions of missing data, while maintaining features not captured by the geostrophic field in regions where both observed winds and thermal data are available.

Other analyses, not shown here, have proven the applicability and versatility of this technique. For example, hemispheric cross sections have been generated which give a more detailed picture of the structure of the polar and subtropical jet streams, along with their associated upper frontal zones. Analyses of lower tropospheric frontal zones have shown characteristics similar to those described by Shapiro and Hastings. Inclusion of radius of curvature information obtained from upper level charts has yielded gradient wind fields which often represent the actual wind field more closely than

do geostrophic approximations. Time sections can also be analyzed yielding much information regarding the temporal evolution of various synoptic features.

4. Summary and conclusions

Objective techniques have been developed to perform analyses of both atmospheric thermal and velocity fields. Using the abundant vertical temperature information available from radiosonde observations, the thermal analysis distinguished regions of both vertical and horizontal gradients. The thermal analysis in turn was used to derive fields of geostrophic wind, and to enhance the analysis of the normal component of the observed wind.

The availability of such an objective analysis routine, including a thermally consistent analysis of the observed wind, could aid greatly both the operational forecaster and the research meteorologist. The speed of the technique and the thermal constraints applied to the wind analysis eliminate many of the previous drawbacks to the use of cross sections in real time situations, making available another important forecast tool.

In research, the technique allows much versatility. Depending on data availability and the purpose of the study, consistent analyses involving the thermal field and the observed, geostrophic and gradient wind fields are possible. It will also be possible to calculate various derived parameters; such as Richardson number, potential vorticity, etc., as suggested by Shapiro and Hastings. The speed of the analysis technique also allows the analysis of a large number of cross sections. This ability could prove invaluable in assessing the credibility of data being made available from satellite soundings both now and in the future.

5. Acknowledgements

The authors wish to thank Prof. Lyle Horn for his inspiration in this work, and Louis Uccellini for his many experiments using the analysis programs. Amy Alexander must also be thanked for her assistance in the final manuscript. This research was supported by National Oceanic and Atmospheric Administration (Meteorological Satellite Laboratory) grant number 04-4-158-2 and National Science Foundation grant number DES74-05814.

Appendix A

The distance between two points on the earth along a great circle route is easily computed from spherical trigonometry. Defining,

A = 90° - (latitude of point 1)

B = 90° - (latitude of point 2)

C = (longitude of point 2) - (longitude of point 1),

the distance in angular measure between points 1 and 2 is

$$d = \cos^{-1} [\cos A \cos B + \sin A \sin B \cos C] .$$

Multiplying by 111.1 gives an approximate distance in kilometers.

Placement of observations along the cross sectional plane (X_k) is given by

$$X_k = X_n \frac{\sum_{i=2}^{k} d_i}{\sum_{i=2}^{n} d_i}$$

where X_n is the desired length of the analysis area, d_i is the distance between stations i and i-1, and n is the total number of stations. (X_1 and d_1 are equal to zero.)

References

Bleck, R., and Haagenson, P.L., 1968: Objective analysis on isentropic surfaces. NCAR Technical Notes, NCAR-TN-39, Boulder, Colorado, 27 pp.

Danielsen, E.F., 1959: The laminar structure of the atmosphere and its relation to the concept of the tropopause. Arch. Meteor. Geophys. Bioklim, A 11, 293-332.

Duquet, R.T., E.F. Danielsen and N.R. Phares, 1966: Objective cross section analysis. J. Appl. Meteor., 5, 233-245.

Greenspan, D., 1970: Introduction to numerical analysis and applications, Chicago, Markham, 5-12.

Newton, C.W., 1954: Frontogenesis and frontolysis as a three-dimensional process. J. Meteor., 11, 449-461.

Shapiro, M.A., and J.T. Hastings, 1973: Objective cross-section analyses by Hermite polynomial interpolation on isentropic surfaces. J. Appl. Meteor., 12, 753-762.

Intercomparisons of Data Derived from Nimbus-5 Satellite Soundings, Radiosonde Observations and Initialized LFM Model Fields

Lyle H. Horn, Ralph A. Petersen and Thomas M. Whittaker
Department of Meteorology, University of Wisconsin-Madison, Wisconsin 53706

Abstract

A 23-24 February 1975 case study is made comparing the results achieved using Nimbus-5 satellite sounding data with those obtained from radiosonde data and the initial hour data of the Limited Area Fine Mesh (LFM) model of the National Meteorological Center. An objective analysis technique is used to construct and analyze isentropic cross sections through an intense baroclinic zone. The cross section based on 17 UT Nimbus-5 soundings is compared with those based on 12 UT and 00 UT radiosonde and LFM data. Geostrophic shear calculations are used to compare the thermal gradients for various isobaric layers obtained from the three data sets. The Nimbus-5 data give results which show somewhat less detail than those based on the radiosonde data, but more than obtained from the LFM data. The RMS differences between the geostrophic shear derived from the Nimbus data and those obtained from the radiosonde data are no greater than those between the radiosonde and LFM data sets. Comparisons of the mean temperatures in various isobaric layers for the three time periods indicate that the 17 UT Nimbus data give results that appear to be consistent with the changing synoptic pattern. Estimates of the wind components normal to the cross sections are obtained using: 1) the geostrophic wind

calculated from the Nimbus-5 data, 2) the observed winds which are enhanced by the geostrophic shear obtained from the radiosonde data and 3) the initial hour LFM winds. Good agreement is noted between the three sets of wind estimates. In general, the results suggest that the insertion into numerical models of satellite derived mean thermal gradients calculated for 100-200 mb thick layers, rather than mean temperatures, may facilitate the use of satellite soundings.

1. Introduction

During the past several years, major advances have been realized in retrieving atmospheric temperature profiles from infrared and microwave irradiance measurements made from satellites. The use of these new data has great potential for producing significant improvement in numerical weather predictions. Undoubtedly, the major contribution of satellite soundings will be to provide observations in regions of the earth where conventional radiosonde data are very sparse. In addition, the finer horizontal mesh of satellite soundings may also detect smaller scale weather producing systems not always captured by the conventional network. Before the potential of these new data can be realized a number of problems must be resolved. The general characteristics and accuracy of the satellite soundings must be assessed, since the mixing of these data with conventional data may introduce an element of shock to a model which offsets the advantage provided by the additional data. Since most of the satellite data are asynoptic, the problem of assimilating the data is also crucial. Of additional importance is the establishment of a reference level pressure on which to build the geopotential height field. These problems are currently being attacked. As Haltiner and Williams (1975) have noted, it is reasonable to expect that the coupling of temperature soundings derived from satellites with additional surface observations, such as from buoys, will largely compensate for the lack of soundings in data-void areas.

Late in 1972, the Nimbus-5 satellite was launched. Aboard it were the Infrared Temperature Profile Radiometer (ITPR) offering high horizontal

spatial resolution (35 km), and the Nimbus-E Microwave Spectrometer (NEMS) offering improved soundings in cloudy areas. In this paper we shall examine the ability of soundings, derived from measurements made by these experimental instruments, to resolve the thermal field in a strong baroclinic zone over the United States. The examination centers on comparisons of vertical cross sections made from various data sources in the neighborhood of the frontal zone. Nimbus-5 temperature data were used to construct an isentropic cross section and to calculate the components of the geostrophic wind shear normal to the cross section through the thermal wind relationship. By assuming that the 850 mb geostrophic wind was known, estimates of the geostrophic wind component perpendicular to the cross section were also obtained. Similar cross sections, constructed from radiosonde temperature and wind data, were used as a standard with which to compare the satellite derived data. Comparisons were also made with cross sections constructed from the initial hour data of the Limited Area Fine Mesh (LFM) model of the National Meteorological Center (NMC). Although the LFM initial hour data are based primarily on the radiosonde observations, the initialization procedure modifies the data to make it suitable for the model calculations, generally smoothing the representation. A comparison between the LFM initial hour and the satellite sounding data can thus provide some insight as to how acceptable data of the Nimbus-5 quality may be as input for the LFM model. Before considering the difficult problem of assessing the quality of the satellite data, a brief review of the Nimbus-5 sounding system will be given.

2. The Nimbus-5 ITPR and NEMS Sounders

Nimbus-5 was launched on 11 December 1972 in a sun-synchronous orbit, inclined at an angle of 80° to the equator. The orbit was

nearly circular with an elevation of about 1100 km. The ITPR instrument measures infrared radiation in seven spectral intervals, four being within the 15 μm CO_2 band. Assuming that the distribution of the absorbing gases is known and that the atmosphere is cloudless, radiation in a spectral interval near the center of an absorption band is emitted from high altitudes while that in the wings of the band is emitted from lower altitudes. Planck's law, which relates the intensity of the radiation to temperature, can be used to infer the temperature profile from the various radiation measurements.

In areas of partial cloud cover, observations made simultaneously in two window regions (3.7 and 11 μm) aid in defining clear column radiances. Because the two window channels respond equally to a uniform opaque surface but unequally to a non-uniform surface, cloudy and clear areas can be detected. The variation in the radiance in one window channel with respect to the other is used to extrapolate the observations to equivalent values for cloudless conditions. With the establishment of the clear column radiance for the window region, the clear column radiance for any of the sounding channels can be specified. Since the ITPR instrument has a field of view of only 35 km, clear columns can be obtained in areas of considerable cloud cover, although not in regions of solid overcast. The ITPR was designed to scan left and right of the orbital track. Unfortunately, since the scan mechanism malfunctioned early in its life, the ITPR soundings used here were derived from only nadir data.

The NEMS instrument measures thermal radiation in five regions of the microwave portion of the spectrum. Only the three channels in the 0.5 cm oxygen band are used to retrieve temperature profiles. The spatial

resolution of about 200 km is considerably larger than that of the ITPR instrument; however, clouds have little effect on the microwave observations. In fact, the NEMS instrument is capable of sensing to the surface even through an overcast. Only the presence of clouds with a large liquid water content, typically precipitating cells, causes any significant attenuation. Staelin et al. (1975) have noted that clouds have affected less than 0.5 percent of the NEMS temperature profiles. See The Nimbus-5 User's Guide, 1972 for further descriptions of the ITPR and NEMS instruments.

The Nimbus-5 temperature profiles are obtained from the radiances using a "minimum information" inverse solution of the radiative transfer equations. Since a number of different temperature profiles could fit a given set of irradiance measurements, some type of first guess profile is needed to narrow the search for a solution. A large historical sample of radiosonde and rocketsonde profiles has been used to establish corresponding theoretical radiances. These radiances then have been used by the National Environmental Satellite Service (NESS) to calculate the coefficients for the regression model from which the guess profile is obtained. See Smith et al., 1970, 1972.

Amalgamated soundings using both the ITPR and NEMS data are prepared at the Meteorological Satellite Laboratory of NESS. The amalgamated sounding processing technique is centered about the ITPR data, with the NEMS data providing a supporting role where it overlaps with the ITPR measurements. See Smith et al., 1975. The Meteorological Satellite Laboratory has provided the set of amalgamated ITPR and NEMS soundings for the 23 February 1975 case examined in this paper.

3. Assessing the quality of satellite soundings

As noted in the introduction, an assessment of the accuracy of the satellite sounding data is critical to their utility in combination with other data. Misinterpreted, satellite data could cause more harm than good. While such an assessment is of fundamental importance, it is a difficult one since the true thermal structure of the atmosphere is unknown.

Considering the vast experience the meteorological community has gained through radiosonde observations, there is little question that any assessment of satellite derived temperature profiles must be based on their performance compared with radiosonde data as a standard. Yet there are inherent limitations to the ability of the radiosonde to accurately describe the thermal structure of the atmosphere.

During its ascent of nearly one hour duration, a radiosonde package traces out a path that often involves horizontal distances of 100 to 200 km. Thus, it is not unusual for a 200 mb observation to be more than 100 km distant from the 850 mb observation made by the same instrument. Furthermore, the radiosonde observations for one synoptic time are made by about 80 individual instruments in the United States. Even with excellent quality control, differences exist between various packages. Soundings obtained from a satellite platform, on the other hand, are made by one instrument which integrates the upwelling irradiance over a certain field of view; for example, 35 km for the ITPR instrument. Thus, a vertical temperature profile derived from the irradiances represents an integrated value over a 35 km distance. This is usually an advantage for synoptic scale studies. However, there are definite limitations to the satellite soundings: the quality of the retrieval

is to some extent dependent on the first guess profile; the instrument may contain bias errors; the empirical transmission functions must be adjusted; the cloud contamination problem cannot be entirely corrected; and the basic information contained in the upwelling irradiances is insufficient to provide soundings with the same vertical detail obtained by radiosondes. While satellite derived soundings will undoubtedly greatly aid the meteorologist in diagnosing the state of the atmosphere, the radiosonde will in all likelihood remain as the standard for comparison in the foreseeable future.

Several approaches may be used in comparing satellite soundings with conventional radiosonde data. A relatively simple approach is to compare individual satellite retrievals with radiosonde observations made at about the same time and location. Smith et al. (1975), who have compared 90 sets of Nimbus-5 derived temperature profiles with radiosonde observations made within three hours and 225 km of each other, found bias deviations ranging from -2.3°C for the 1000 - 850 mb layer to -0.1°C for the 500 - 400 mb layer (Nimbus-5 colder). The standard deviations ranged from a maximum of 3.0°C for the 1000 - 850 mb and 300 - 250 mb layers to 1.9°C for 150 - 100 mb. Because of the uncertainties in the radiosonde observations themselves these comparisons must be interpreted with caution. In a comparison involving 150 pairs of radiosondes released simultaneously within at most 100 km from each other, RMS differences between the pairs ranged from about 1.3 to 2.3°C in various layers between 1000 and 100 mb (Bengtsson and Morel, 1974). The differences could be caused by several factors: small scale atmospheric variability along the path of the rising balloons, minor deficiencies in the various instruments, round-off errors in the reporting

procedures, etc. Thus, little should be inferred from RMS differences between satellite soundings and radiosondes which are not greater than 1-2°C.

A far more complicated approach to the problem of assessing the quality of satellite soundings is to examine their impact on forecast models. Several studies have employed the Vertical Temperature Profile Radiometer (VTPR) operational soundings. Experiments involving the hemispheric models of NMC and the Goddard Institute for Space Studies indicated that the predictions were, at best, marginally sensitive to the inclusion of VTPR data along with the conventional data (Bengtsson and Morel, 1974). Using the British forecast model, Atkins (1975) reported a similar lack of impact. In a case study, the Swedish Meteorological and Hydrological Institute found that the inclusion of VTPR data produced a somewhat better 500 mb level prediction than that obtained without the satellite data (Bengtsson and Morel, 1974). However, in general the approach of testing the effectiveness of the satellite soundings by including the data into forecast models has been inconclusive. Considering the complexity of this approach, the lack of clear-cut evidence is not surprising. Since satellite data are generally asynoptic, the problem of data insertion becomes critical. Furthermore, the objective analysis techniques, the initialization procedures and the actual iterative steps used by the models under operational conditions could obscure the effect of the satellite data. Studies such as that done by Hayden (1973), who used a relatively simple model and SIRS-B data to carefully study the assimilation of the satellite information, appear to offer considerably more promise in assessing the impact of satellite data than do attempts that lead directly to predictions obtained from the large, complex models.

4. Procedures and Data

Between 1709 and 1718 UT 23 February 1975, Nimbus-5 passed over an intense baroclinic zone over the lower Mississippi Valley. The amalgamated ITPR and NEMS soundings furnished by the Meteorological Satellite Laboratory of NESS were used to construct an isentropic cross section through the baroclinic zone. Temperature retrievals for the mandatory levels (surface, 1000, 850, 700, 500, 400, 300, 250, 200, 150 and 100 mb) were available. An objective analysis program involving overlapping second order Lagrangian polynomials was used in analyzing the thermal field of the cross sections.[1]

Temperature data at the appropriate pressure levels were extracted from the objectively analyzed cross sections and used to evaluate the horizontal temperature gradients. The geostrophic wind shear was obtained from 850 mb upward (and downward) using the thermal wind relationship,

$$U_{Th} = -\frac{R_d}{f} \ln \frac{p_u}{p_\ell} \left(\frac{\partial T}{\partial n}\right) \qquad (1)$$

where U_{Th} is the thermal wind (or geostrophic shear) in the layer between pressure p_u and p_ℓ ($p_\ell > p_u$), T temperature, n horizontal distance (positive toward the right along the cross section), R_d the gas constant

---

[1]The objective analysis program, developed at the University of Wisconsin by Whittaker and Petersen (1975), constructs isentropes between the unevenly spaced stations. Quadratic polynomials are fitted to each set of three adjacent stations, with each polynomial overlapping the adjacent polynomial by one station. A linear combination is used between the overlapping portion of adjacent polynomials. Comparisons with objective analyses based on the program developed by Shapiro and Hastings (1973), give similar results. From the isentropic analysis, values of potential temperature are interpolated to a 40 by 40 grid for use in obtaining thermal gradients.

for dry air, and f the coriolis parameter. The resulting field of geostrophic wind shear perpendicular to the cross section was used for comparisons with similarly derived geostrophic shear fields based on radiosonde temperature observations and LFM initial hour temperature data.[2] As shown in Figure 1, the radiosonde and LFM cross sections had locations nearly identical to the Nimbus-5 orbit.

Comparisons of the geostrophic wind shear fields obtained from the Nimbus-5, radiosonde and LFM data represent comparisons of the horizontal temperature gradients derived from these data sources. This approach lessens the effect of temperature bias errors that may exist in any one data set. By integrating the thermal gradients over isobaric layers, the gradients of the thickness can be calculated for successively deeper layers. If the surface pressure or geopotential height of a single isobaric surface is known, the relative geopotential height fields of other isobaric surfaces can be obtained. The inclusion of a few radiosonde observations (theoretically only one) then permits a description of the geopotential height field. Since numerical models work primarily with the geopotential height of isobaric surfaces, a major test of satellite soundings is their ability to describe the thickness for 100 - 200 mb layers (Bengtsson and Morel, 1974). While radiosonde reports containing all significant level information provide detail of the vertical temperature structure, including sharp inversions, the temperature input to numerical models

---

[2]Since in the calculations 850 mb was used as a base, the shear through any layer is simply the difference between the geostrophic wind value at a level and the value at 850 mb.

consists only of mandatory level data. Consequently, the lack of vertical detail provided by satellite soundings is less crucial than might first be expected.

An additional advantage in expressing the results of the comparisons in terms of geostrophic wind shear is that the components of the actual wind field perpendicular to the cross section can be estimated using the geostrophic wind field constructed from the wind shear and a known wind at a single level. This permits a comparison between the derived geostrophic wind field and the observed wind field obtained from observations of balloon displacements (or possibly cloud elements tracked from a geostationary satellite).

To facilitate comparisons, it was necessary to bracket the Nimbus-5 observations with data obtained from radiosonde observations and LFM initializations prior to and following the satellite passage. Thus the 1709 - 1718 UT 23 February 1975 Nimbus-5 data are compared with the 12 UT 23 February and 00 UT 24 February radiosonde and LFM data.

5. The Synoptic Situation

On 21 February 1975, a major upper tropospheric short wave trough was located over the western United States. During the next two days, the trough amplified and propagated slowly eastward, with some indication that a closed low at 500 mb in the southern portion might completely cut off from the trough to the north. However, the large amplitude trough remained intact, and by 12 UT 23 February 1975, extended from Minnesota south-southwestward into western Texas. The surface trough and frontal system extended from Ohio south-southwestward into the Gulf of Mexico south of Louisiana, with weak frontal waves located over Ohio and Mississippi. Figures 1a and 1b display the surface

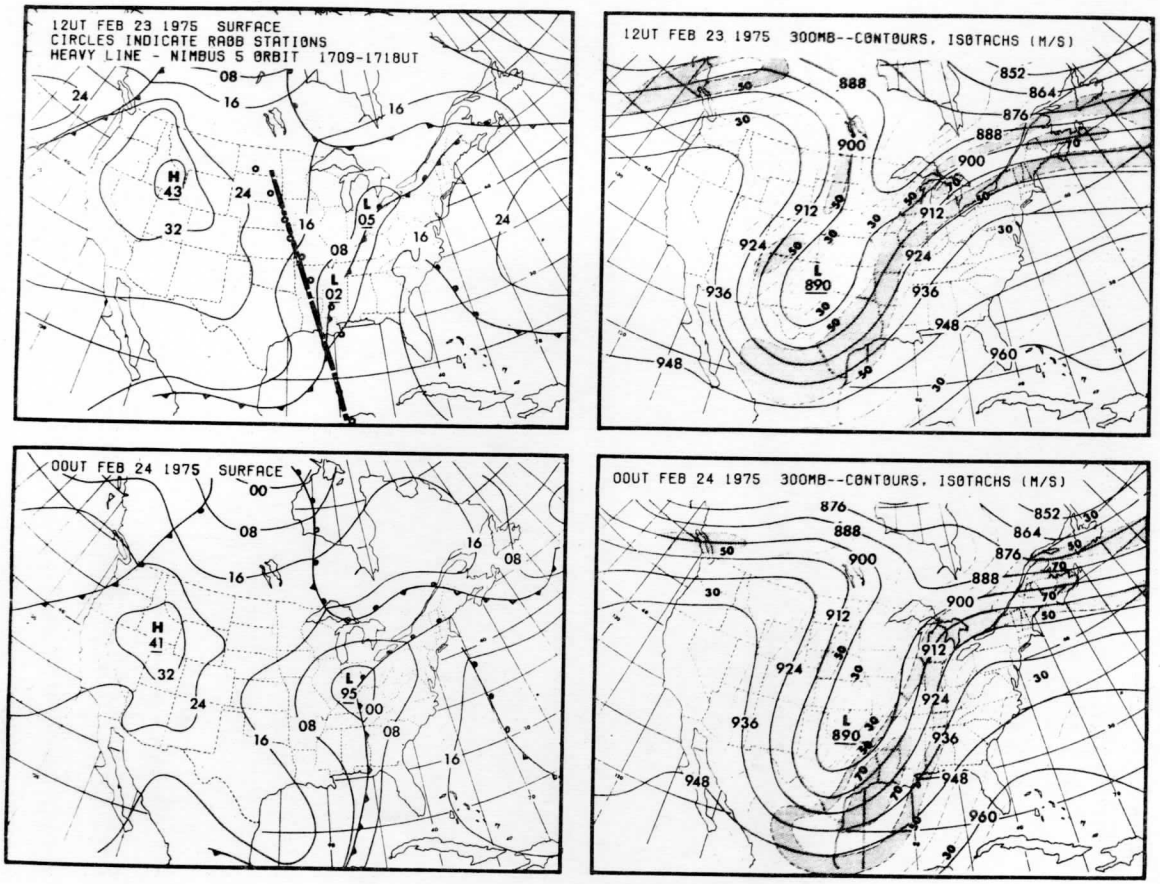

Fig. 1. Surface and 300 mb analyses for 12 UT 23 February 1975 and 00 UT 24 February 1975. Nimbus-5 orbit and radiosonde stations shown in panel A.

and 300 mb charts for 12 UT 23 February 1975. The Nimbus-5 orbit (1709 - 1718 UT) which passed over the frontal zone is superimposed on the surface map (Fig. 1a), and the radiosonde stations which provided conventional data are shown.

During the following twelve hours, the frontal wave over Mississippi developed rapidly into a major cyclone. Its motion was initially northeastward to the Tennessee-Kentucky border by 18 UT 23 February and then northward to southern Indiana by 00 UT 24 February. Figures 1c and 1d show the surface and 300 mb maps for 00 UT 24 February. The 300 mb winds which exceeded 50 m s^{-1} over the lower Mississippi valley at 12 UT 23 February, increased to more than 70 m s^{-1} by 00 UT 24 February. The surface cyclone eventually moved northwestward into central Illinois, having produced a band of heavy snow from northeastern Oklahoma to southwestern Wisconsin.

6. Comparisons between Nimbus-5, radiosonde and LFM data

In comparing the results derived from the Nimbus-5 soundings with the radiosonde and LFM data, three approaches were used. First, intercomparisons were done of the geostrophic shear fields calculated from each of the cross sections. This approach essentially compares the gradients of thickness for successively deeper layers obtained from the three sets of data. Second, layer mean temperature comparisons were done, and finally estimates of the wind field perpendicular to the cross sections were compared.

a. Intercomparisons of geostrophic shear

The isentropic cross sections and geostrophic shear based on Nimbus-5, radiosonde and LFM initial hour data are displayed in Figure 2. 17 UT 23 February Nimbus-5 results are shown twice, in the left

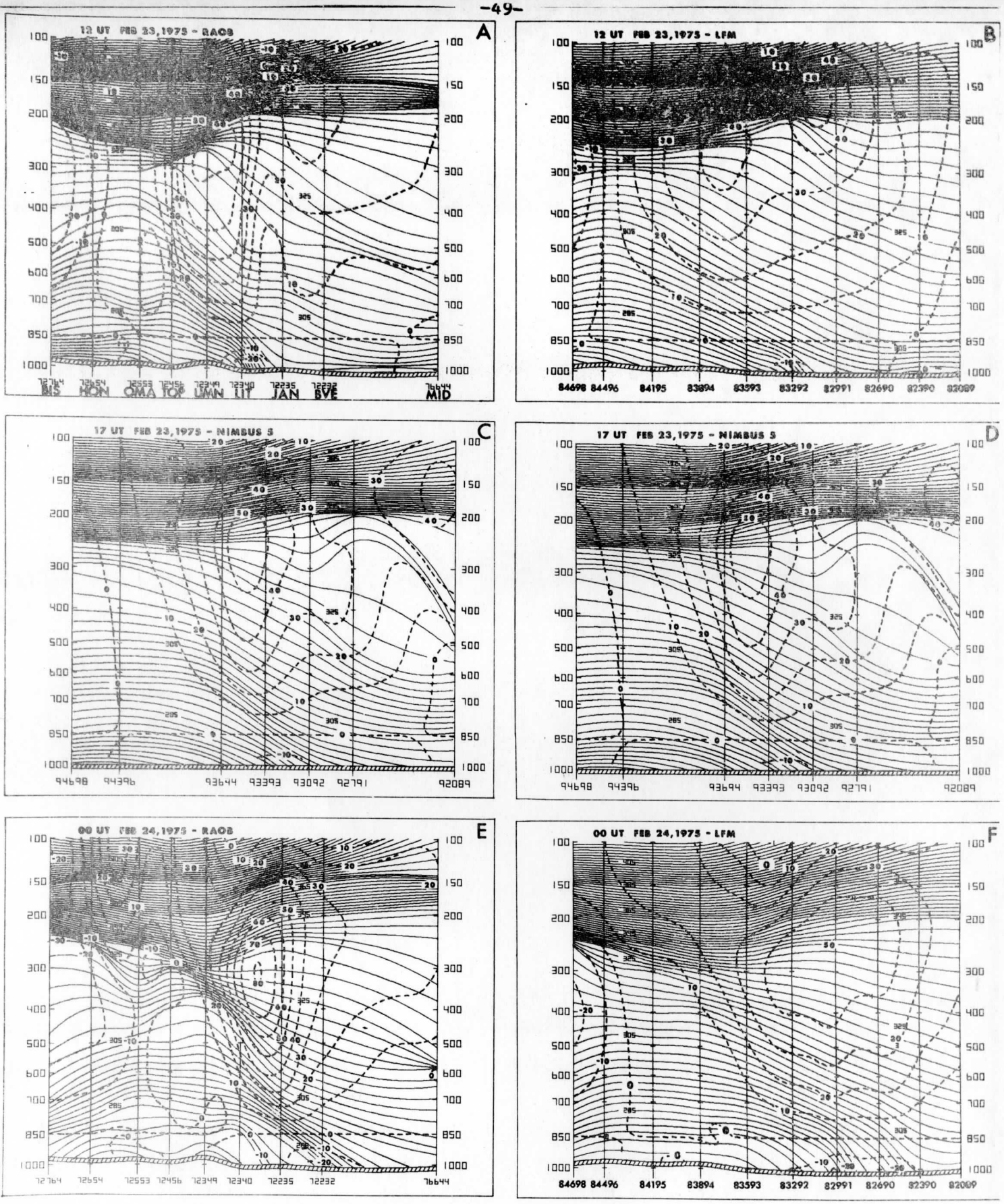

Fig. 2. Vertical cross sections of isentropes (solid lines, 2 K intervals) and geostrophic shear (dashed lines, m s^{-1}). Nimbus-5 UT analyses are repeated in panels C and D to facilitate comparisons with 12 UT and 00 UT radiosonde analyses (A and E) and LFM analyses (B and F).

column they are bracketed by the raob results for 12 UT 23 February and 00 UT 24 February, and in the right column by the LFM results for these same times. The cross sections are positioned so that a given latitude is located at an equivalent position in each panel. The locations of the Nimbus-5 soundings are given in terms of their latitude and longitude, preceded by a 9 (e.g., 94698 is a sounding centered near 46°N, 98°W). The block and station numbers of the radiosonde stations are shown below each data point (e.g., 72764 is block 72 station 764, Bismarck, N.D.). Only mandatory level data were used. The numbers below the LFM grid points are their latitude and longitude preceded by an 8. These initial hour data, obtained from operational tapes provided by the Data Assimilation Branch of NMC, are taken from a diagonal of the LFM grid which falls almost exactly along the Nimbus-5 orbit shown in Figure 1.

A visual comparison of the results displayed in Figure 2 indicates that, in general, the isentropes and geostrophic shear based on the radiosonde data show the greatest detail, even though only mandatory level data were used in their construction. The isentropes and shear of the LFM initial hour data display the smoothest fields. The Nimbus-5 results have detail between those of the radiosonde and LFM data, but are closer to the LFM. All three sets capture the strong baroclinic zone, with the radiosonde data greatly emphasizing its intensity.

For the 12 UT 23 February time period, there is a marked difference between the LFM and radiosonde results. Both show a double core of shear, but in the radiosonde section the more northerly (and lower) core is much stronger (68 m s^{-1}) than the southern one (35 m s^{-1}). In the LFM section the reverse is true, with the more northerly core having

a maximum of 44 m s^{-1} versus 56 m s^{-1} for the southern core. For the later synoptic period (00 UT) both the LFM and radiosonde sections have a single maximum of shear, although the LFM core is broader and weaker. The smoothing present within the LFM cross section is largely responsible for the differences. In the 12 UT radiosonde section the baroclinity is concentrated between stations 72349 and 72235, while in the LFM the region of baroclinity is spread more uniformly over a much greater north-south extent. When working with models based on the primitive equations, smoothing is especially necessary to insure computational stability. It should also be noted that the LFM initial hour output, as well as forecast output, is given for ten levels, but is obtained from six sigma layers. Thus some additional vertical smoothing is inherent in the output procedure.

The Nimbus-5 section, which represents observations taken about midway between the two synoptic times, positions the core of shear at about the same latitude and altitude as the radiosonde sections, although of weaker intensity. Between the 12 UT and 00 UT observations, the core of radiosonde shear shifted slightly southward and downward. The 17 UT Nimbus-5 core is located not far from the midpoint of these two positions. The weaker intensity of the Nimbus-5 core is probably due in part to the poorer vertical resolution of the individual satellite soundings and also to the fact that two satellite soundings (39°N, 95°W and 23°N, 95°W) were discarded because they showed obvious signs of being seriously cloud contaminated.[3] A check of the surface weather

---

[3] In the objective cross section analysis used here, the isentropes are required to fit the observed data exactly. Consequently, erroneous data are more readily revealed than they would be if the observed data were interpolated to a fixed grid. In this event the erroneous data could have been camouflaged by inherent smoothing during interpolation to grid points.

in the region of the discarded soundings showed heavy overcast and steady precipitation. If the discarded sounding at 39°N, 95°W had been usable, it may have added data which could have increased the intensity of the shear core. This is a deficiency of satellite soundings.

In comparing the Nimbus-5 cross section with the two LFM sections which bracket it, the somewhat smoother fields of the LFM data are noted. Although the maximum shear values for all three sections (12, 17 and 00 UT) are about the same, the LFM shear maxima are located above deep layers of uniform baroclinity, while in the Nimbus-5 sections the baroclinity is concentrated in more limited layers. The maximum shear in the LFM data is also displaced to the south of that in the satellite sections. In these respects, the Nimbus-5 results are more like the radiosonde analyses.

The RMS differences of the geostrophic shear calculated from the three sources of data are shown in Figure 3. The results are graphed for successively thicker layers (850 - 700 mb, 850 - 500 mb,..., 850 - 100 mb). Intercomparisons were done for shears calculated from the 17 UT Nimbus-5 data and each of the other four analyses. RMS differences were also calculated between the 12 UT and 00 UT radiosonde and LFM shears to provide some knowledge of the atmospheric variations which occurred between the two synoptic times. Furthermore, in doing the RMS intercomparisons, the data were divided into two sets. One was based on data from the entire cross section (46-20°N), while the other set used data from only the core of the shear (40-27°N). It is in this core region of strong thermal gradients that the ability of the Nimbus-5 data to resolve the thermal field is put to its severest test. The RMS values are expressed in m s^{-1}, and for two layers (850 - 500 mb and

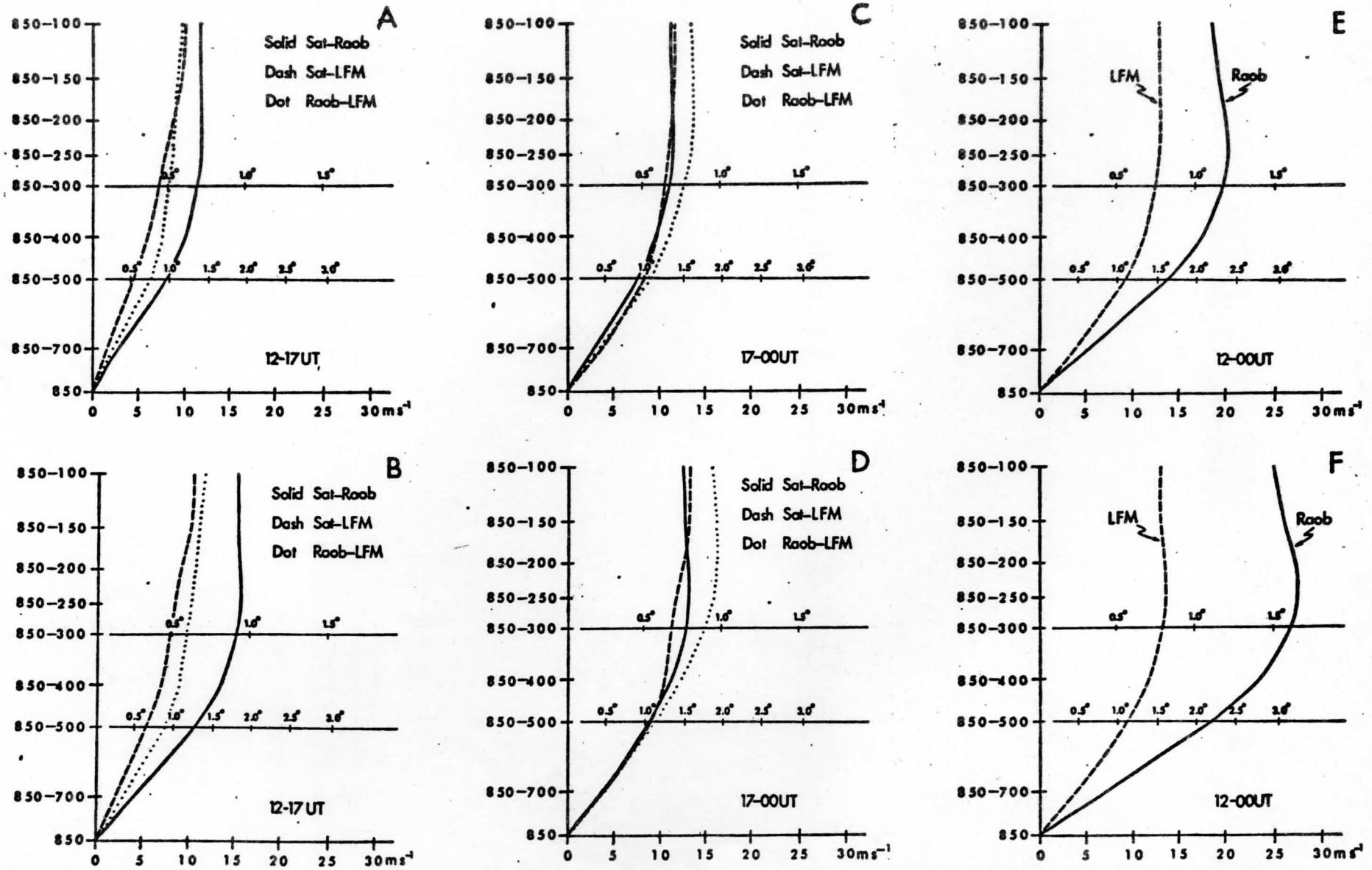

Fig. 3. Intercomparisons of cumulative geostrophic shear expressed as RMS differences. Top panels are based on the entire cross section (46-20°N); bottom panels for the core of baroclinity (40-27°N). A and B are comparisons between 17 UT Nimbus and 12 UT raob and LFM data; C and D same except using 00 UT raob and LFM data. Solid lines Nimbus - raob; dashed line Nimbus - LFM; dotted line raob - LFM. Panels E and F display RMS differences between 12 UT and 00 UT raob and LFM data. Equivalent RMS differences expressed in layer mean temperature gradients (°C/222 km) are shown in scales at the 500 and 300 mb levels. See text.

850 - 300 mb) in terms of the gradients of the mean temperature (°C/222 km). In calculating the equivalent thermal gradients a constant value of the coriolis parameter (f) for latitude 34° was assumed.

The intercomparisons of the 12 UT radiosonde and LFM data and the 17 UT Nimbus data show that the largest RMS differences are between the radiosonde and Nimbus data, reaching a maximum of 15 - 16 m s^{-1} at 250 mb in the core region (Fig. 3b). However, at 300 mb a 15 m s^{-1} shear is produced by only a 0.9°C/222 km mean temperature gradient in the 850 - 300 mb layer. In the core region, the RMS differences between the Nimbus-5 data and LFM data are somewhat less than between the radiosonde and LFM data. For the whole cross section the 12 UT - 17 UT RMS differences (Fig. 3a) are smaller than for the core region, but with the largest differences again between the satellite and radiosonde data.

The 17 UT - 00 UT intercomparisons (Figs. 3c, 3d) differ considerably from the 12 UT - 17 UT values. The cumulative RMS differences for the satellite - radiosonde comparisons are only about two-thirds as large as the 12 UT - 17 UT values. Furthermore, of the three intercomparisons, the smallest cumulative RMS differences are generally between the radiosonde and Nimbus data. As noted earlier this is probably the result of the rapid development of the cyclone after 12 UT, so that by 17 UT 23 February the gradients were probably more like those at 00 UT 24 February than at 12 UT 23 February. For 00 UT the largest RMS differences are between the radiosonde and the LFM data. Since the radiosonde observations are the major source of the LFM data, this may seem surprising. However, the smoothing that is done in the initialization procedure can lead to rather major differences in the shear fields. When comparing a cross section of initialized LFM data with a nearly

coincident cross section based on the raw radiosonde data, it should be kept in mind that the LFM results are based on more than just the stations along the cross section. The NMC objective analysis uses the 6-layer Primative Equation (PE) model forecast made twelve hours earlier as a first guess. Then the Cressman (1959) technique of circular searching is used to assign weights to the radiosonde observations in the vicinity of a grid point.

The right two panels (Figs. 3e and 3f) illustrate the changes that were observed between 12 UT 23 February and 00 UT 24 February. The cumulative RMS differences between the radiosonde data for the two synoptic times are much larger than those between the 17 UT Nimbus data and either 12 UT or 00 UT radiosonde data. Similarly, the differences between the geostrophic shears calculated from the two LFM synoptic times are larger than the RMS differences between the 17 UT Nimbus data and either of the LFM data periods. It is interesting to see that the cumulative RMS differences between the two radiosonde data sets are considerably larger than between the two LFM sets. This is a further illustration of the smoothing inherent during the LFM initialization.

In order to examine the differences between the three sets of data within discrete isobaric layers, RMS differences of the mean temperature gradients in the individual layers were calculated. The intercomparisons expressed in °C/222 km are presented in Table I. Again, the calculations were done for the entire cross section and separately for the region of greatest baroclnity. The values based on the entire cross section range from a maximum of 2.3°C/222 km (00 UT LFM versus 17 UT Nimbus) to several values equal to or less than 0.7°C/222 km for the various intercomparions. For the limited cross section the values range

from 2.4 to 0.4°C/222 km. It is noteworthy that the RMS differences between the satellite derived temperature gradients and those obtained from the radiosonde or LFM data are not significantly different from those between the radiosonde and LFM data sets. This is encouraging, especially since the satellite passage occurred at a time five to seven hours different from the synoptic times.

TABLE 1

RMS differences of layer mean temperature gradients (°C/222 km) for individual layers. Columns at left intercompare 12 UT Raob, 12 UT LFM and 17 UT Nimbus-5 Data. Columns at right intercompare 00 UT RAOB, 00 UT LFM and 17 UT Nimbus-5 data. First values are for the entire cross section (46° - 20°N). Values in parentheses are for the core of the baroclinic region (40° - 27°N).

LAYER	12 UT Raob vs 17 UT Nimbus	12 UT LFM vs 17 UT Nimbus	12 UT Raob vs 12 UT LFM	00 UT Raob vs 17 UT Nimbus	00 UT LFM vs 17 UT Nimbus	00 UT Raob vs 00 UT LFM
850-700 mb	1.7(2.3)	0.9(1.2)	1.3(1.6)	1.8(2.3)	2.3(2.4)	2.2(2.3)
700-500	1.7(2.2)	1.1(1.2)	1.2(1.4)	1.6(1.7)	1.2(1.3)	1.5(1.7)
500-400	1.0(1.0)	0.8(0.6)	0.6(0.6)	1.7(2.1)	0.6(0.6)	1.3(1.7)
400-300	1.1(0.5)	1.2(0.7)	0.4(0.4)	1.8(1.7)	1.1(0.6)	1.4(1.4)
300-250	1.4(1.4)	1.7(1.7)	0.8(1.1)	2.2(2.4)	1.6(1.3)	1.4(1.6)
250-200	1.6(1.8)	1.8(2.1)	1.1(1.3)	2.1(2.1)	1.6(1.8)	1.1(1.5)
200-150	0.7(1.0)	0.6(0.6)	1.0(1.2)	1.4(1.4)	1.5(1.6)	1.1(1.3)
150-100	0.7(0.7)	0.9(1.1)	0.9(1.1)	0.9(1.1)	0.8(0.9)	0.6(0.6)

b. Intercomparisons of layer mean temperatures.

For the same layers we used for temperature gradient comparisons, Smith et al. (1975) calculated RMS temperature differences ranging from 3.1 to 1.9°C for 90 pairs of Nimbus-5 and radiosonde soundings made within 225 km and three hours of each other. Despite the much smaller data sample for the 23-24 February 1975 case studied, we did a similar comparison. The results are presented in Table 2. The bias differences calculated for the various intercomparisons shown are simply the algebraic differences between two data set means. The differences were calculated using either 19 or 38 pairs of grid points obtained from the cross section depending on whether the core or the entire cross section was used for the computations. Because the 17 UT Nimbus-5 soundings were made between the 12 UT and 00 UT observation times, all possible intercomparisons were made involving the three times. The bias and RMS differences for the 90 pairs of observations studied by Smith et al. (1975) are included at the far right of the table and repeated in both the upper and lower parts of the table.

The comparisons shown in Table 2 should be treated with caution since the synoptic pattern changed quite rapidly between 12 UT February 23 and 00 UT February 24. This is illustrated by the change in the bias differences in the core region between the 17 UT Nimbus - 12 UT radiosonde and the 17 UT Nimbus - 00 UT radiosonde comparisons. For the first time interval the Nimbus-5 850-700 mb temperatures were 2.0°C colder than the 12 UT radiosonde values; however, for the 17 UT-00 UT comparison the satellite values were 4.9°C warmer than the radiosonde. This change is simply a reflection of the 6.9°C cooling observed in the radiosonde temperatures between 12 UT and 00 UT. The fact that

LAYER	12UT-17UT				12UT		17UT-00UT				00UT		12UT-00UT				From Smith et al.	
	SAT-RAOB		SAT-LFM		RAOB-LFM		SAT-RAOB		SAT-LFM		RAOB-LFM		RAOB-RAOB		LFM-LFM			
(mb)	BIAS	RMS	BIAS	RMS	BIAS	RMS	BIAS	RMS	BIAS	RMS	BIAS	RMS	BIAS	RMS	BIAS	RMS	BIAS	RMS
850-700	1.0	2.0	0.8	1.6	0.2	1.3	2.9	3.9	3.6	5.1	0.8	2.4	3.9	5.8	4.2	6.1	-1.3	2.8
700-500	0.4	1.8	-0.2	1.4	0.7	1.1	1.9	2.7	2.7	3.3	0.8	1.8	2.3	4.0	2.4	3.5	-0.9	2.7
500-400	-0.0	1.0	-0.8	1.1	0.8	0.9	1.2	2.0	1.4	1.5	0.3	1.3	1.2	2.4	6.0	1.3	-0.1	2.1
400-300	-0.1	0.8	-0.0	0.8	-0.1	0.2	-0.3	1.1	-0.5	0.7	-0.2	0.9	-0.4	1.0	-0.4	0.7	-0.5	2.8
300-250	-0.0	1.1	0.6	1.5	-0.6	0.8	-1.9	2.5	-2.2	2.5	-0.3	0.9	-1.9	3.1	-1.5	2.4	-0.9	3.1
250-200	0.2	1.3	0.6	1.7	-0.4	0.7	-2.7	3.4	-3.5	3.9	-0.7	1.2	-2.6	3.7	-2.8	3.9	-1.0	2.8
200-150	-0.4	0.5	-0.0	0.5	-0.3	0.7	-1.5	2.1	-2.2	2.6	-0.7	1.0	-1.8	2.3	-2.1	2.8	-0.4	2.2
150-100	-0.3	0.7	-0.1	0.7	-0.2	0.6	-0.6	1.1	-0.4	0.8	0.2	0.5	-0.9	1.1	-0.5	0.7	-0.1	1.9
850-700	2.0	2.8	1.6	1.9	0.4	1.6	4.9	5.3	6.3	6.9	1.4	3.1	6.9	7.9	7.9	8.4	-1.3	2.8
700-500	1.5	2.4	0.8	1.5	0.8	1.3	2.8	3.1	3.8	4.1	1.1	2.3	4.3	5.3	4.6	4.8	-0.9	2.7
500-400	0.6	0.9	-0.3	0.6	0.9	0.9	1.8	2.6	1.8	1.9	-0.1	1.6	2.4	3.3	1.6	1.7	-0.1	2.1
400-300	-0.4	0.6	-0.4	0.5	-0.1	0.3	0.1	1.1	-0.3	1.1	-2.4	3.0	-0.3	1.1	-0.6	0.7	-0.5	2.8
300-250	-0.9	1.3	-0.3	1.1	-0.5	0.7	-2.4	3.0	-2.6	2.7	-0.2	1.0	-3.2	4.1	-2.9	3.3	-0.9	3.1
250-200	-0.6	1.3	-0.5	1.5	-0.2	0.6	-3.8	4.2	-4.6	4.7	-0.9	1.5	-4.4	5.0	-5.1	5.5	-1.0	2.8
200-150	-0.4	0.6	-0.3	0.5	-0.1	0.7	-2.5	2.7	-3.4	3.5	-0.9	1.3	-2.9	3.0	-3.7	3.9	-0.4	2.2
150-100	-0.3	0.5	-0.2	0.5	-0.2	0.8	-1.1	1.2	-0.7	0.8	0.4	0.6	-1.4	1.5	-0.9	0.9	-0.1	1.9

TABLE 2. Various bias (°C) and RMS (°C) intercomparisons of 17 UT Nimbus-5 and radiosonde and LFM layer mean temperatures for 12 UT and 00 UT. Top portion of table for entire cross section; lower part for baroclinic core. Values on far right (repeated in upper and lower portions) are from Smith et al. (1975) who compared 90 approximately co-located Nimbus-5 and radiosonde soundings.

850 mb-700 mb layer temperature obtained from the 17 UT Nimbus data has a value between the 12 UT and 00 UT radiosonde values is encouraging. Above about 400 mb there is a reversal in the bias difference with the 17 UT Nimbus warmer than the 12 UT raob and LFM values, but colder than 00 UT raob and LFM temperatures. This trend for cooling in the lower troposphere and warming aloft is typical of rapid baroclinic development and is revealed clearly in the differences between the 12 UT and 00 UT raob and LFM data. Apart from the synoptically explainable differences there is probably some residual bias. In using satellite soundings, it is common to find a bias in one direction at lower levels but the opposite direction at upper levels, although the mean temperature over a deep layer (e.g. 1000-200 mb) is well described.

RMS differences of the geostrophic shear between the 17 UT Nimbus and 12 UT radiosonde and LFM data were greater than between the 17 UT and 00 UT data. The RMS differences in the layer mean temperatures show the opposite trend; for example, in the 850-700 mb layer the RMS value is 2.8°C for the comparison between the 17 UT Nimbus and 12 UT radiosonde data, but 5.3°C for the 17 UT - 00 UT comparison. Even though the geostrophic shear patterns obtained from 17 UT Nimbus-5 resemble the 00 UT radiosonde and LFM patterns more than the 12 UT patterns, the tightening of the gradients by 00 UT led to larger RMS differences between the temperatures.

c Intercomparisons of normal wind components

Several studies have been done in which the geostrophic wind components derived from the satellite soundings have been compared with those obtained from radiosonde data. Using simulated data to reconstruct the thermal field beneath a jet core, Togstad and Horn (1974) found that

in a cloudless atmosphere an infrared soundings of high accuracy are very capable of describing the thermal field in a hyperbaroclinic zone. Smith et al. (1975) have used Nimbus-5 soundings to obtain the geostrophic wind components perpendicular to cross sections in the western Pacific for three February 1974 cases and in the eastern Atlantic for a May 1974 case. Their results showed a good correlation with the observed and geostrophic winds derived from radiosonde data. Kapela and Horn (1975) compared derived geostrophic and gradient wind components normal to cross sections based on ITPR, NEMS, and amalgamated ITPR and NEMS soundings with observed winds, and also with the geostrophic and gradient winds calculated from radiosonde data. They too obtained favorable results.

In this study, we have intercompared the wind components normal to the cross section obtained from the three data sets. The results are shown in Figure 4. For the radiosonde cross sections, corner left panels of Fig. 4, the wind components perpendicular to the cross section were obtained using a combination of the observed wind reports at the mandatory levels and the thermal wind relationship. The geostrophic shear was calculated at each of the 40 by 40 grid points on the objectively analyzed cross sections. Through a series of vertical and horizontal interpolations a wind field was achieved which has isotachs that fit the observed wind components at the mandatory levels of the reporting stations and also uses the thermal gradient information to enhance the details of the wind field at the 40 by 40 grid points which do not coincide with an observation. We have labeled this wind field the thermally enhanced observed winds. It was felt that this approach would provide the best estimate of the actual wind components perpendicular to the cross section. Since in this case study, the contours at the various

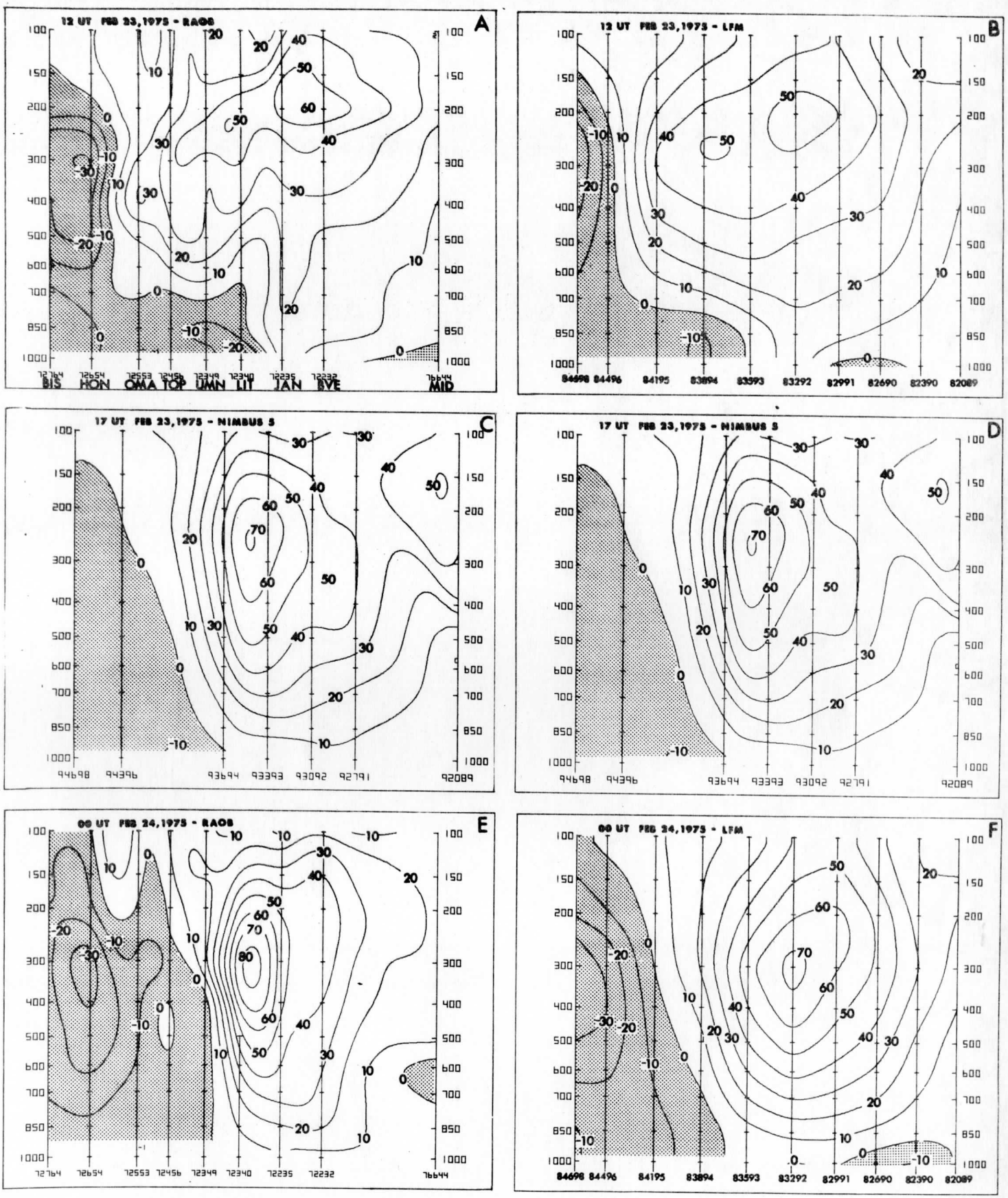

Fig. 4. Normal components of wind estimates obtained from radiosonde, Nimbus-5 and LFM sources (m s^{-1}). Panel arrangement same as in Fig. 2.

isobaric levels had very little curvature, no attempt was made to add a gradient wind correction.

The wind components normal to the Nimbus-5 cross section (center panels) were estimated using the values of the geostrophic shear and the 850 mb geostrophic wind calculated from the NMC analyses of the 850 mb charts as a base. Since the satellite passage occurred about midway between the 12 UT 23 February and 00 UT 24 February sounding times, the average of the 850 mb geostrophic wind at these two times was used.

The LFM cross sections were constructed from the initial hour wind data. In the initialization process, the divergent component of the objectively analyzed wind field is removed during the relaxation process and replaced by the divergent component from the previous 12-hour PE forecast. This divergent component is then added to the non-divergent component of the objectively analyzed winds to obtain the initial hour wind field. It is the normal component of this wind field that we have displayed in the LFM cross sections shown in the corner right panels.

Recall that the calculations of the geostrophic shear (Figure 3) showed a marked difference between the radiosonde and LFM results for 12 UT. Their wind fields (Figs. 4a and 4b), however, appear quite similar. The LFM wind field is somewhat smoother than the thermally enhanced radiosonde wind field, but the double cores of maximum winds have comparable locations and intensities in both cross sections. The largest difference appears in the negative components near the northern edge of the cross sections. In general, differences between the two are likely due to the LFM objective analysis and initialization.

The 17 UT Nimbus-5 geostrophic wind field closely resembles the 00 UT LFM and thermally enhanced wind fields, indicating the rapid cyclogenesis that occurred in the five hours following 12 UT. Of the three isotach fields the LFM field (Fig. 4f) is the smoothest, with the Nimbus-5 field (Fig. 4d) being nearly as smooth. Both have maximum winds in excess of 70 m s^{-1}. The 00 UT thermally enhanced observed wind field (Fig. 4e) shows the greatest detail and strongest winds in the jet core. At 00 UT the winds at Little Rock (72340) were not reported above 500 mb, so the intensity of the jet core above that level was determined through the thermal enhancement procedure. Since the upper level charts for 00 UT show the core of the polar jet near Little Rock (72340), it is likely that the balloon was lost because of the low tracking angle.

The wind estimates derived from Nimbus-5 show a secondary maximum (50 m s^{-1}) at about 165 mb over the southern Gulf of Mexico. A similar maximum is not found on any of the other cross sections. Since there are no radiosonde stations along this portion of the cross section it was not possible to explicitly verify the existence of this wind maxima. However, movie loops from the Syncronous Meteorological Satellite (SMS-1) for 23 February 1975 show a cirrus shield over the southern Gulf of Mexico, a position consistent with the existence of a subtropical jet in this region. An independent assessment by Parmenter (1976) based on several individual SMS-1 pictures supports this view.

A major purpose of intercomparisons between the wind fields is to test the ability of the Nimbus-5 soundings to resolve a thermal field which can then be used to adequately locate a jet core. The results displayed in Figure 4 indicate that in this case the Nimbus-5

sounder did quite well. In Table 3, the latitude, altitude and intensity of the jet cores obtained from the three sets of data are summarized. The 17 UT data furnished by Nimbus-5 appear to fit nicely between the 12 UT and 00 UT observations.

TABLE 3

Comparisons of the jet core obtained from the three data sets. (For the 12 UT time the stronger of the two cores was used).

TIME	DATA SET	LAT(°N)	ALT.(mb)	SPEED ($m\ s^{-1}$)
Feb. 23, 1975	12 UT Enhanced Obs. Winds	31.5	200	60
Feb. 23, 1975	12 UT LFM Initial Hour	32.0	200	57
Feb. 23, 1975	17 UT Nimbus-5	34.5	255	71
Feb. 24, 1975	00 UT Enhanced Obs. Winds	34.5	310	84
Feb. 24, 1975	00 UT LFM Initial Hour	32.0	300	75

7. Conclusions

Although temperature profiles obtained from satellites will eventually play a major role in providing input data for numerical weather prediction models, a number of difficult problems concerning the application of the satellite soundings are yet to be resolved. In this study we have chosen to investigate one of the problems, namely the quality of the satellite data. A case study approach was used involving intercomparisons between data obtained from 1) radiosonde observations, 2) the initial hour output of the LFM model of NMC and 3) Nimbus-5 amalgamated infrared and microwave soundings. Thermal gradients obtained from isentropic cross sections of the three sets of data were expressed and compared in terms of the geostrophic wind shear. Comparisons were also made between the mean temperatures for various isobaric layers between 850 and 100 mb. In addition, the observed winds obtained from radiosonde observations were enhanced using the thermal wind equation and compared with the initial hour winds of the LFM model and the geostrophic winds calculated from the Nimbus-5 data. The 23-24 February 1975 case was chosen because Nimbus-5 data for that period were available and also because an especially intense baroclinic zone was present to provide a severe test for the Nimbus-5 soundings. Because the satellite passage occurred about midway between radiosonde observation times, the satellite data were intercompared with radiosonde and LFM data from the observation times preceding and following the satellite passage.

The Nimbus-5 soundings were retrieved by the National Environmental Satellite Service using a minimum information inverse solution of the radiative transfer equations. This procedure employs a first guess solution obtained from regression coefficients calculated from a historical

sample of radiosonde and rocketsonde temperature profiles and their corresponding theoretical radiances. Thus, the Nimbus-5 soundings are entirely independent of the radiosonde data used in this study.

The intercomparisons of the geostrophic shear obtained from the three data sources indicate that the Nimbus-5 soundings did quite well in describing the intense baroclinic zone. RMS differences of the geostrophic shear calculated from the different data sets for successively thicker layers show that the differences between the radiosonde and LFM initial hour data for the same time period were often as great or greater than the differences between the Nimbus-5 and the radiosonde or LFM data. For the 850 - 300 mb layer the RMS difference between the shear from the Nimbus data and that calculated from either the radiosonde or LFM data was equivalent to a RMS difference in the mean temperature gradient in the layer of less than 1.0°C/222 km. The RMS differences in mean temperature gradients for individual isobaric layers ranged between 2.4°C/222 km and 0.4°C/222 km.

Intercomparisons of the mean temperatures for individual isobaric layers provided results which appear to be consistent with the changing synoptic conditions between 12 UT and 00 UT. Bias differences between the 12 UT-17 UT data sets and between 17 UT-00 UT data suggest that the Nimbus-5 data provided a reasonable description of the thermal field at 17 UT. Relatively large RMS temperature differences exist between the 17 UT and 00 UT data, despite the fact that the geostrophic shear and wind patterns obtained from the 17 UT Nimbus data more closely resemble the 00 UT radiosonde and LFM patterns than the 12 UT data. This is likely due to the strengthening of the temperature gradients between 12 UT and 00 UT, thus making larger RMS temperature differences possible.

The intercomparisons between the Nimbus-5, radiosonde and LFM data were extended to include the wind fields normal to the cross sections. These results were also encouraging, with the 17 UT Nimbus-5 geostrophic wind field fitting nicely between the 12 UT and 00 UT radiosonde and LFM wind fields. Because the three wind fields were obtained using different methods a detailed intercomparison did not seem appropriate.

Although the 17 UT Nimbus mean temperatures within individual isobaric layers seem reasonably representative of the actual conditions, it appears that the major reason for the positive results obtained in this study is that the intercomparisons were chiefly based on gradients obtained separately from the three data sets. This lessens the effect of any bias errors which might exist between the satellite and radiosonde temperature observations. While it is indeed encouraging to find that the Nimbus-5 data possess good relative accuracy, it must be noted that their successful employment in numerical models requires that they be mixed with conventional data. The results of this study suggest that efforts should be increased to incorporate isobaric layer mean temperature gradients obtained from the satellite observations with the conventional data. Such an approach may optimize the use of satellite sounding data as input to numerical models. Since the Nimbus-5 data were confined to nadir observations, it was not possible to work with horizontal fields of data. However, the scanning infrared and microwave instruments aboard Nimbus-6 provide such data.

While there is much work to be done before the full promise of the satellite sounding data can be realized, one must be encouraged in viewing results such as those showing the normal wind components (Fig. 4). Had the major trough and cyclogenesis of the 23-24 February 1975 case occurred over the relatively data-void Atlantic or Pacific, observations of the Nimbus-5 quality could have provided extremely valuable input to the numerical prediction models.

8. Acknowledgements

The authors wish to thank William L. Smith and William C. Shen of NESS for providing the Nimbus-5 soundings, and Hugh O'Neil of the Data Assimilation Branch of NMC for furnishing copies of the LFM tapes. They also gratefully acknowledge the fine assistance of Thomas Koehler, Amy Alexander, Richard Hyde and Eva Singer in preparing the manuscript and figures. The comments of Christopher M. Hayden concerning the manuscript were also most helpful. This study was done through support provided by the Meteorological Satellite Laboratory of the National Environment Satellite Service under NOAA Grant 04-4-158-2.

References

Atkins, M. J., 1975: The value of Satellite Vertical Temperature Profile Radiometer (VTPR) data in numerical weather prediction. Invited paper presented at XVI General Assembly, International Union of Geodesy and Geophysics, Grenoble, France.

Bengtsson, L., P. Morel, 1974: The performance of space observing systems for the first GARP global experiment, GARP Working Group on Numerical Experimentation, Report No. 6.

Cressman, G., 1959: An operational objective analysis system. Mon. Wea. Rev., 103, 367-374.

Haltiner, G. J., and R. T. Williams, 1975: Some recent advances in numerical weather prediction. Mon. Wea. Rev., 103, 571-590.

Hayden, C. M., 1973: Experiments in four-dimensional assimilation of Nimbus-4 SIRS data. J. Appl. Meteor., 12, 425-436.

Kapela, A., and L. H. Horn, 1975: Nimbus-5 satellite soundings in a strongly baroclinic region, Meteorological Applications of Satellite Indirect Soundings, Project Report, NOAA Grant 04-4-158-2, Dept. of Meteorology, University of Wisconsin, Madison.

Nimbus-5 User's Guide, Goddard Space Flight Center, Greenbelt, Md., 1972.

Parmenter, F., 1976: Personal Communication, Applications Group, National Environmental Satellite Service.

Shapiro, M. A., and J. T. Hastings, 1973: Objective cross-section analyses by Hermite polynomial interpolation on isentropic surfaces. J. Appl. Meteor., 12, 753-762.

Smith, W. L., H. M. Woolf, and W. J. Jacob, 1970: A regression method for obtaining real-time temperature and geopotential height profiles from satellite spectrometer measurements. Mon. Wea. Rev., 98, 582-603.

Smith, W. L., H. M. Woolf, and H. E. Fleming, 1972: Retrieval of atmospheric temperature profiles from satellite measurements for dynamical forecasting.

J. Appl. Meteor., 11, 113-122.

Smith, W. L., H. M. Woolf, C. M. Hayden and W. C. Shen, 1975: Nimbus-5 Sounding Data Processing System Part II: Results Final Report, NASA Contract S-70249-AG.

Staelin, D. H., A. L. Cassel, K. F. Kunzi, R. L. Pettyjohn, R. K. L. Poon, and P. W. Rosenkranz, 1975: Microwave atmospheric temperature sounding: effect of clouds on the Nimbus-5 satellite data.

J. Atmos. Sci., 32, 1970-1976.

Togstad, W. E., and L. H. Horn, 1974: An application of the satellite indirect sounding technique in describing the hyperbaroclinic zone of a jet streak. J. Appl. Meteor., 13, 264-276.

Whittaker, T. M., and R. A. Petersen , 1975: Objective cross section analysis incorporating thermal enhancement of the observed winds, Meteorological Applications of Satellite Indirect Soundings, Project Report, NOAA Grant 04-4-158-2, Dept. of Meteorology, University of Wisconsin, Madison.